https://doi.org/10.5194/egusphere-2023-2557
Preprint. Discussion started: 8 November 2023

Revising VOC emissions speciation improves global simulations of ethane and propane

Matthew J. Rowlinson[1,2], Lucy J. Carpenter[2], Katie A. Read[1,2], Shalini Punjabi[1,2], Adedayo Adedeji[2], Luke Fakes[2], Ally Lewis[1,2], Ben Richmond[3], Neil Passant[3], Tim Murrells[3], Barron Henderson[4], Kelvin H. Bates[5,6], Detlev Helmig[7], and Mat J. Evans[1,2]

[1]National Centre for Atmospheric Science, University of York, York, YO10 5DD, UK
[2]Wolfson Atmospheric Chemistry Laboratories, Department of Chemistry, University of York, York, YO10 5DD, UK
[3]Ricardo, Fermi Avenue, Harwell, Oxon, OX11 0QR, UK
[4]United States Environmental Protection Agency, Research Triangle Park, Durham, North Carolina 27709, USA
[5]NOAA Chemical Sciences Laboratory, Boulder, CO, 80305, USA
[6]Cooperative Institute for Research in Environmental Sciences, University of Colorado, Boulder, CO, 80305, USA
[7]Boulder A.I.R. LLC, Boulder, CO 80305, USA

Correspondence: Matthew J. Rowlinson (matthew.rowlinson@york.ac.uk)

Abstract. Non-Methane Volatile Organic Compounds (NMVOCs) generate ozone (O_3) when they are oxidized in the presence of oxides of nitrogen, modulate the oxidative capacity of the atmosphere and can lead to the formation of aerosol. Here, we assess the capability of a chemical transport model (GEOS-Chem) to simulate NMVOC concentrations by comparing ethane, propane and higher alkane observations in remote regions from the NOAA Flask Network and the World Meteorological Organization's Global Atmosphere Watch (GAW) network. Using the Community Emissions Data System (CEDS) inventory we find a significant underestimate in the simulated concentration of both ethane (35%) and propane (64%), consistent with previous studies. We run a new simulation where the total mass of anthropogenic NMVOC emitted in a grid box is the same as that used in CEDS, but with the NMVOC speciation derived from regional inventories. For US emissions we use the National Emissions Inventory (NEI), for Europe we use the UK National Atmospheric Emissions Inventory (NAEI), and for China, the Multi-resolution Emission Inventory for China (MEIC). These changes lead to a large increase in the modelled concentrations of ethane, improving the mean model bias from -35% to -3.8%. Simulated propane also improves (from -64% to -48.0% mean model bias), but there remains a substantial model underestimate. There were relatively minor changes to other NMVOCs. The low bias in simulated global ethane concentration is essentially removed, resolving one long-term issue in global simulations. Propane concentrations are improved but remain significantly underestimated, suggesting the potential for a missing global propane source. The change in the NMVOC emission speciation results in only minor changes in tropospheric O_3 and OH concentrations.

1 Introduction

Volatile Organic Compounds (VOCs) play a central role in the chemistry of the atmosphere. Methane dominates much of this chemistry, due to its large emissions from both natural and anthropogenic activities (Kirschke et al., 2013), while a comparable

https://doi.org/10.5194/egusphere-2023-2557
Preprint. Discussion started: 8 November 2023

mass of isoprene (C_5H_8) is also emitted globally by the biosphere (Guenther et al., 1995). However, other non-methane volatile organic compounds (NMVOCs) such as alkanes, alkenes, aromatics, alcohols, carbonyls are also emitted into the atmosphere by both natural and anthropogenic processes (Simpson et al., 1999; Li et al., 2017b; Hoesly et al., 2018). Following oxidation, NMVOCs contribute to the formation of tropospheric ozone (O_3), a pollutant with detrimental effects on both climate and human health (Monks et al., 2015; Szopa et al., 2021b), and impact the global oxidative capacity through changes to the OH concentration (Fry et al., 2012). Some NMVOCs also contribute to the production of secondary organic aerosols (Hodzic et al., 2016).

Ethane and propane are two of the most globally abundant NMVOCs. Atmospheric concentrations and trends in ethane and propane are controlled by the balance of their emissions, which are predominantly anthropogenic (Aydin et al., 2011; Simpson et al., 2012; Helmig et al., 2014) and their major loss by reaction with the OH radical. Previous modelling studies have underestimated the atmospheric concentrations of ethane and propane by as much as a factor of two for ethane, and perform even worse for propane (Pozzer et al., 2007; Dalsøren et al., 2018; Emmons et al., 2015). As there is no secondary chemical production of ethane and propane, the low bias must be the result of underestimated emissions or an overactive sink. Previous studies have concluded that the underestimate is primarily due to an underestimate in anthropogenic emissions inventories (Carmichael et al., 2003; Pozzer et al., 2007; Tzompa-Sosa et al., 2017; Dalsøren et al., 2018; Emmons et al., 2015). Possible explanations for this underestimate range from missing natural emissions sources (Etiope and Ciccioli, 2009; Dalsøren et al., 2018), a mis-representation of the rapid increases in industrial emissions (Franco et al., 2016), and/or broad underestimates in bottom-up anthropogenic inventories (Pozzer et al., 2010; Dalsøren et al., 2018).

Emissions inventories have a number of uses, from regulatory compliance to use in chemical and climate modelling. The latter can be used in the assessment of the air quality or climate policies. Priority is often given to species with a direct impact on air quality (NO_x, SO_2) or to greenhouse gases (CO_2, CH_4) rather than species such as NMVOC which are often seen as being of secondary importance. Global inventories, such as the Community Emissions Data System (CEDS) (Hoesly et al., 2018) aggregate local, country-based emission estimates where available, to build a global emission data set based on the best estimates from regional data. The CEDS emissions estimates use total emissions of NMVOCs from regional inventories, such as the European Monitoring and Evaluation Programme (EMEP) (EMEP/CEIP, 2021), the National Emissions Inventory in the USA (US-EPA, 2021) or the Multi-resolution Emission Inventory model for Climate and air pollution research (MEIC) in China (Li et al., 2017a). CEDS then speciates the total NMVOCs emissions into 25 VOC classes by country and sector, based on estimates from the RETRO project (Koffi et al., 2016; McDuffie et al., 2020). This speciation is time invariant and does not reflect possible temporal trends in emission ratios.

In response to the underestimated ethane and propane in global models, attempts have been made to improve emissions of these species with new inventories (Tzompa-Sosa et al., 2017; Xiao et al., 2008), based on model inversions of the observations. These indicate substantially higher rates of emissions than the bottom up estimates, however, they are often annually invariant and don't have widespread use given a community preference for bottom-up rather than top-down estimates.

Here we explore the causes of the model underestimate of ethane and propane in chemical transport models, and assess the effect of alternative regional NMVOC speciations. We assess the performance of current global emissions inventories

https://doi.org/10.5194/egusphere-2023-2557
Preprint. Discussion started: 8 November 2023

for NMVOCs, contrasting those simulations with those using re-speciated NMVOC emissions based on regional emissions estimates. In Section 2, we describe the configuration of the chemical transport model used, the observations used for model evaluation and the regional and global emission inventories used. In Section 3, we describe the default model simulation of NMVOCs using the CEDS emissions. Section 4 describes the process of improving the default emissions using the NMVOC speciation from the regional inventories and Section 5 evaluates model performance following its application and explores the impact of these changes on atmospheric oxidation.

2 Model and Observations

2.1 GEOS-Chem

All simulations were completed using the 3-D global chemical transport model GEOS-Chem, version 14.0.1 (Bey et al., 2001) (www.geos-chem.org; **10.5281/zenodo.7383492**). The model was driven by MERRA-2 meteorology from the NASA Global Modeling and Assimilation Office (Gelaro et al., 2017), with 72 vertical levels and a spatial resolution of 2.0°×2.5°. All simulations were run for 3 years from 2015. The first year is considered spin-up and the model output is then compared to observations for the years 2016 and 2017. The model used an updated chemical mechanism with improved benzene, toluene and xylene oxidation chemistry, described by Bates et al. (2021). The model used biomass burning emissions from GFED4s (van der Werf et al., 2017) and biogenic emissions from MEGAN v2.1 (Guenther et al., 1995).

Global anthropogenic emissions in GEOS-Chem are typically provided by the Community Emissions Data System (CEDS) (Hoesly et al., 2018), which is one of the most widely used inventories for anthropogenic emissions in atmospheric modelling studies (McDuffie et al., 2020). CEDS emissions are initially based on country level estimates of emissions obtained from regional efforts such as the EMEP, which are accumulated to create a global gridded emissions inventory. CEDS emissions are therefore closely related to the regional inventories that they are built upon. Small differences emerge during the processing from re-gridding and differing treatments of particular sectors. For NMVOCs in particular there can be large differences between CEDS and regional inventories, due to the method of speciating NMVOCs. Regional emissions of total NMVOCs are used in CEDS to calculate global emissions, before then being speciated to produce emissions for individual VOCs. This has the advantage of providing a consistent methodology for speciation globally, but means that emissions of individual NMVOC species will be different between the regional and global estimates. During this speciation of NMVOCs substantial discrepancies can emerge between CEDS and the national inventories such as the NEI in the USA (Figure 9).

The higher alkanes (butanes, pentanes and hexanes) are lumped in GEOS-Chem to a single tracer (ALK4), therefore CEDS emissions of the higher alkanes are also lumped to create a comparable mass emission. GEOS-Chem uses the OH rate constant of butane for ALK4, however the rate constants for pentanes and hexanes are substantially different (generally around 2 times faster) (Atkinson et al., 2006). As a result, we would expect GEOS-Chem to overestimate ALK4 concentrations as the chemical sink in the model is slower than in reality.

A number of studies have identified geological emissions of ethane and propane as an important, often neglected source (Dalsøren et al., 2018; Etiope and Ciccioli, 2009; Nicewonger et al., 2016). This source of ethane is estimated at 2.0-4.0 Tg yr^{-1} by

https://doi.org/10.5194/egusphere-2023-2557
Preprint. Discussion started: 8 November 2023

Etiope and Ciccioli (2009), similar in magnitude to the estimate of preindustrial emissions in Nicewonger et al. (2016). This makes up 10-20% of the total present-day annual emission from all sources. Propane emissions from geological sources are estimated at 1.0-2.4 Tg yr^{-1}, larger than the propane source from biomass burning and making up 10-25% of total present-day emissions (Dalsøren et al., 2018). Therefore, we include geological emissions in this study, with a fixed annual emission of 3.0 Tg of ethane, and 1.7 Tg of propane. The spatial distribution of these emissions is based on gridded CH_4 geological emissions data (Etiope et al., 2019), which estimates locations of methane emissions from 4 geological sectors; onshore seeps, submarine seeps, microseepages and geothermal manifestations. The emissions are emitted continuously with no temporal variation.

2.2 Observations

Observational datasets of surface VOC concentrations are limited compared to other species such as O_3, CO or NO_x (Carpenter et al., 2022). We therefore use two contrasting datasets to evaluate the modelled concentrations; the NOAA global flask network (Helmig et al., 2021) and observations made by sites from the World Meteorological Organisation (WMO), Global Atmospheric Watch (GAW) network (WMO, 2021). Figure 1 shows the distribution of these sites. The NOAA sites are split into 6 geographical regions as part of the analysis (Figure 1).

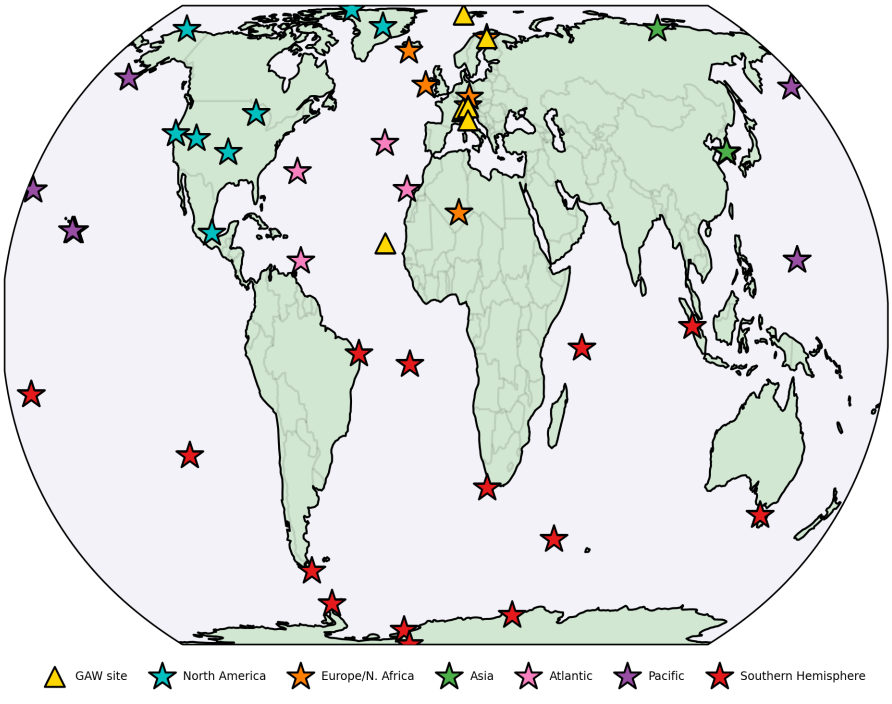

Figure 1. Locations of GAW measurement sites and NOAA flask collection sites. The NOAA sites have been divided into 6 key regions for the evaluation, shown by the colours of the symbols.

https://doi.org/10.5194/egusphere-2023-2557
Preprint. Discussion started: 8 November 2023

2.2.1 NOAA flask datasets

The National Oceanic and Atmospheric Administration (NOAA) and the Institute of Arctic and Alpine Research (INSTAAR) in Boulder, Colorado, operated a global VOC monitoring network established in 2004 based around flask sampling (Helmig et al., 2021). VOCs measurements were taken weekly or bi-weekly at 44 sites considered to be representative of the global background. The measurements were sampled in pairs from glass flasks. The NMVOC analysis is performed after the measurement of greenhouse gases and methane stable isotopic ratios.

The NMVOCs are measured by gas chromatography with flame ionization detection, calibrated by a series of gravimetrically prepared synthetic and whole air standards. The programme operates under the umbrella of the World Meteorological Organization Global Atmospheric Watch (WMO-GAW) and collaborates with international partners on exchange of calibration standards and comparison of calibration scales. The INSTAAR laboratory was audited by the World Calibration Center (WCC) for VOCs in 2008 and 2011. Five unknown standards were analysed and results reported to the WCC. Mean results of five repeated measurements of the provided standards deviated by <1.5% for ethane and <0.8% for propane from the certified values. These deviations are well within the criteria set by GAW. Uncertainties in the hydrocarbon data are estimated to be $\leq$5% for mixing ratios of >100 pptv, and $\leq$5 pptv for mixing ratios <100 pptv. For this study, 43 sites providing measurements over the relevant period were used in evaluating the model results.

Here, we use the measurements of ethane and propane and the sum of iso-butane, n-butane, iso-pentane and n-pentane concentrations as 'higher alkanes' to allow comparison with the GEOS-Chem ALK4 tracer. Data from 2016 and 2017 is used to evaluate the model performance.

2.2.2 WMO-GAW datasets

The WMO-GAW network has measurement sites in more than 80 countries, providing measurements of a range of compounds relevant to climate and air quality (WMO, 2021). However, NMVOC measurements are not made at all GAW sites. The available datasets relevant to this study represent a small subset of GAW sites, and are entirely located in Europe or the North Atlantic (see Figure 1). In this study, 2016 and 2017 measurements are used.

3 Base model performance

The model performance was evaluated by running its standard configuration using CEDS anthropogenic emissions for ethane, propane, and the higher alkanes, plus geological emissions of ethane and propane. The simulated mass-weighted global mean tropospheric [OH] is 1.06 $\times 10^6$ molec cm^{-3}, within the estimated range from other chemistry models (Naik et al., 2013; Voulgarakis et al., 2013). The modelled tropospheric methane lifetime is 9.3 years, also within the expected range (Prather et al., 2012; Szopa et al., 2021a). Root-mean squared error (RMSE = $\sqrt{\frac{\sum_{i=1}^{n}(P_i-O_i)^2}{N}}$) between the model and the measurements is shown for each region. We also use a normalised mean bias (NMB = $\sum_{i=1}^{n}(P_i-O_i)/\sum_{i=1}^{n}O_i$) metric to assess model performance.

https://doi.org/10.5194/egusphere-2023-2557
Preprint. Discussion started: 8 November 2023

3.1 Ethane

Figure 2 shows the comparison between measurements of ethane concentrations made as part of the NOAA flask network and those calculated by the model, divided into 6 regions. Orthogonal distance regression (Boggs and Donaldson, 1989) was used to calculate the line of best fit. The model underestimates ethane concentrations in all 6 regions shown in Figure 1, with an overall bias of -35.0%. The greatest NMB was found at measurements in the Atlantic (-48.6%), with the lowest at Asian sites (-18.7%). However, the largest absolute error was seen at Asian sites with a RMSE of 880 ppt, indicating poor model skill despite the smaller bias. At Asian, European and Atlantic sites, the underestimate appears more pronounced for higher concentrations, indicated by the slope of the line of best fit. The error appears to be lower in the southern hemisphere, where measured concentrations tend to be lower, however, there remains a model bias of -32.0%.

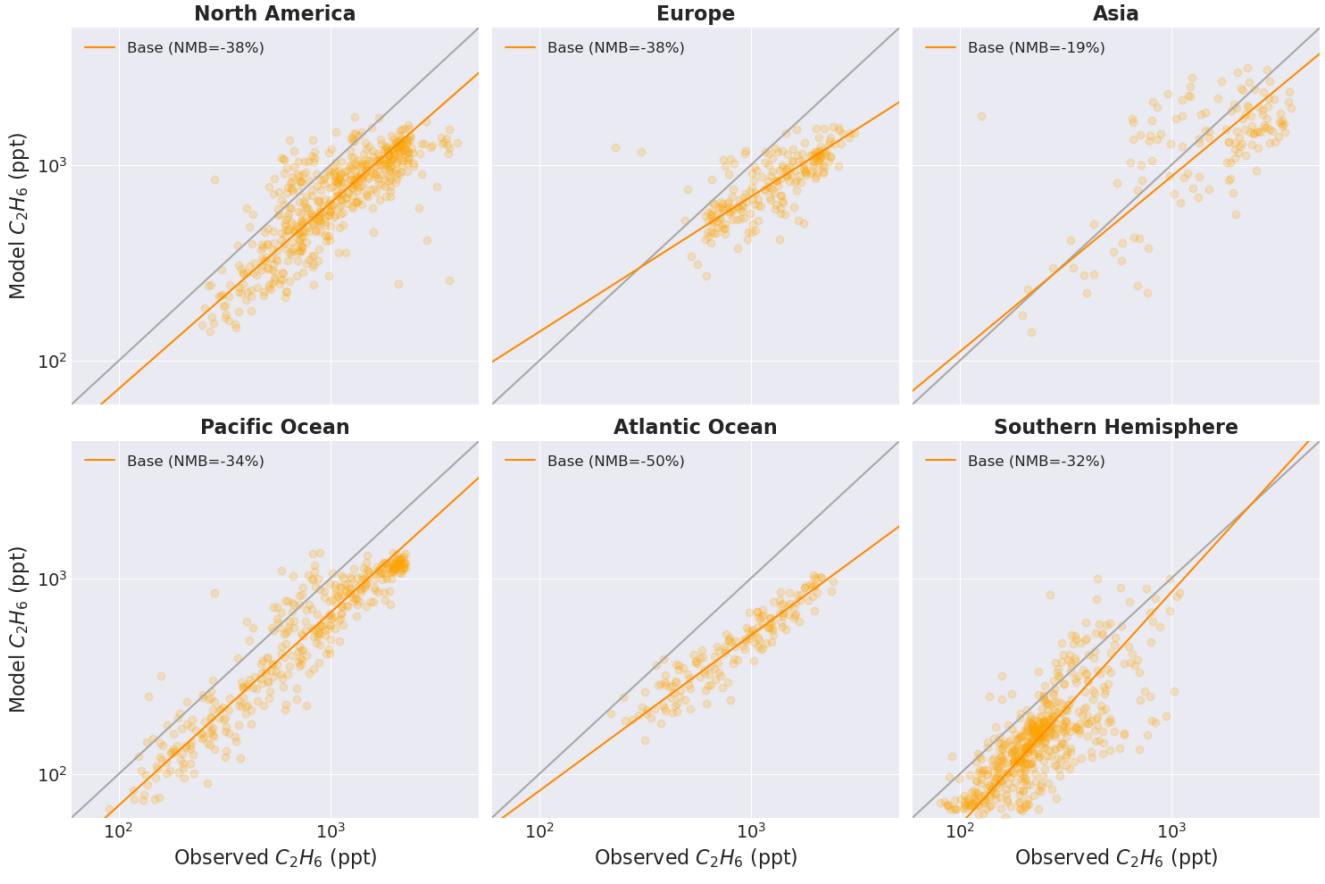

Figure 2. Modelled and observed hourly mean ethane concentrations in ppt. Simulated concentrations are compared to observed values for 43 NOAA Flask network sites for the years 2016-2017 (see Figure 1). An orthogonal distance regression (orange line) and 1 to 1 regression (grey) are also included.

https://doi.org/10.5194/egusphere-2023-2557
Preprint. Discussion started: 8 November 2023

Figure 3 shows simulated and observed ethane at the 7 GAW sites. Consistent with the flask data, the simulated ethane is underestimated in the model at all 7 sites, with an overall low bias of -38.2%. The RMSE ranges from 540 ppt to 776 ppt across the sites, with greater error at sites situated above 1000m altitude. In the summer months at Cape Verde, Hohenpeissenberg and Zeppelin there tends to be better agreement in absolute values between model and observations when concentrations are lower. However, winter and spring values are underestimated by as much as a factor of 2 at all sites. Overall the model simulation of ethane is consistent with previous modelling studies (Carmichael et al., 2003; Pozzer et al., 2007; Etiope and Ciccioli, 2009; Pozzer et al., 2010; Franco et al., 2016; Tzompa-Sosa et al., 2017; Dalsøren et al., 2018), with concentrations broadly underestimated by a factor of 2 across both flask measurements and GAW sites.

https://doi.org/10.5194/egusphere-2023-2557
Preprint. Discussion started: 8 November 2023

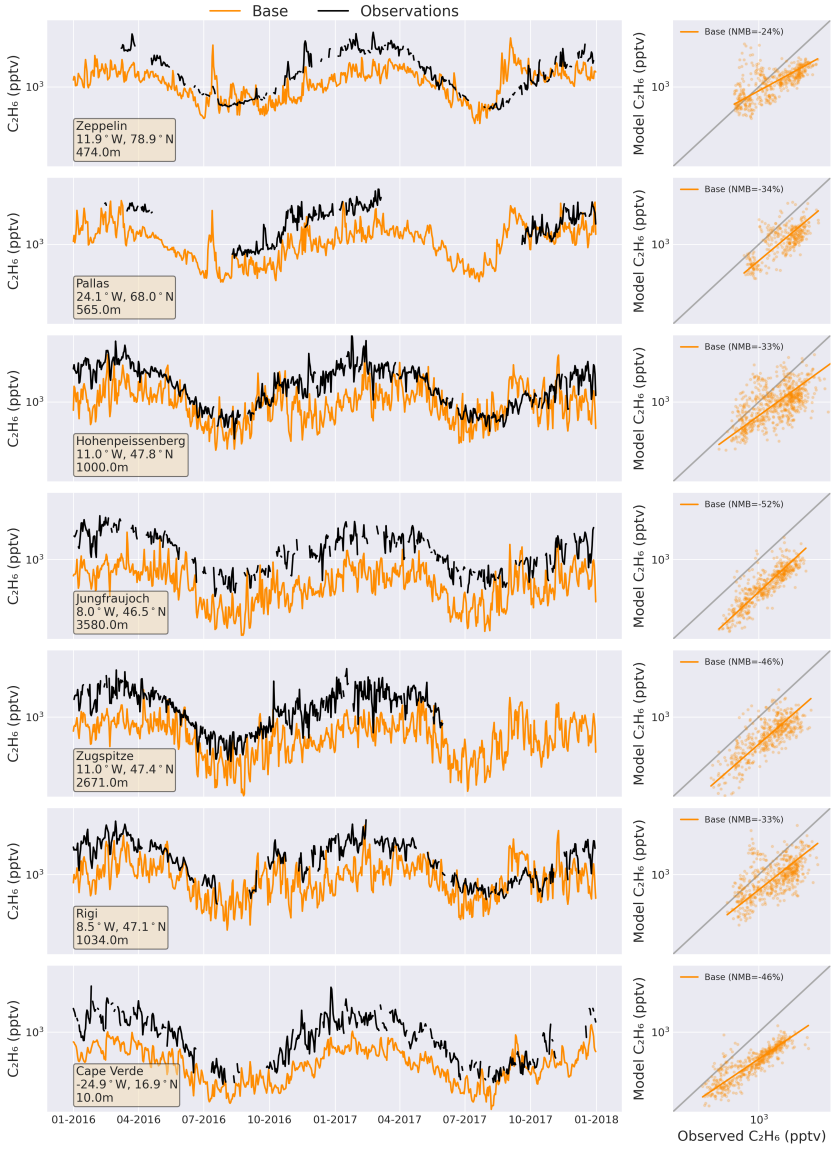

Figure 3. Observed (black line) daily mean concentrations of ethane at 7 GAW sites compared with simulated concentrations using default CEDS emissions (orange).

3.2 Propane

Figure 4 shows the comparison between the modelled simulation of propane and the measurements made at the NOAA flask sites. Like ethane, propane concentrations are substantially underestimated in the model, with a bias across all sites of -63.8% and -59.2% for the NOAA and GAW datasets, respectively. Measurements from Asia have the largest error with a RMSE of 788 ppt and bias of -48.8%, although there is significant scatter. Over the oceans and Southern Hemisphere the RMSE ranges

https://doi.org/10.5194/egusphere-2023-2557
Preprint. Discussion started: 8 November 2023

from 130 to 261 ppt, with the model often underestimating by more than a factor of 2, with a bias up to 80.0% in the Southern Hemisphere and Atlantic regions.

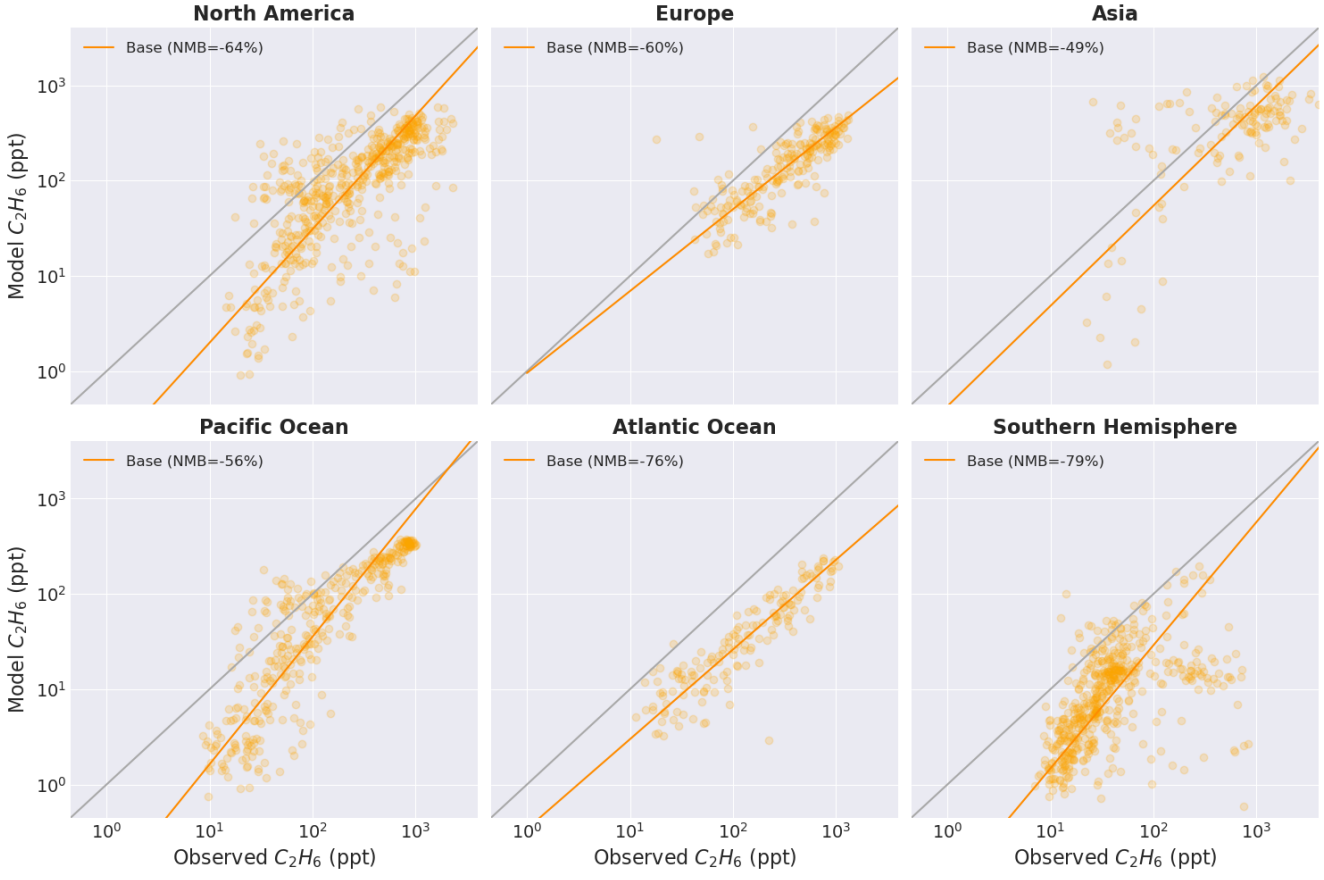

Figure 4. Modelled and observed hourly mean propane concentrations in ppt. Simulated concentrations are compared to observed values for 43 NOAA Flask network sites for the years 2016-2017 (see Figure 1). An orthogonal distance regression (orange line) and 1 to 1 regression (grey) are also included.

155 The simulated propane concentrations compare similarly with the measurements at GAW sites across Europe and Cape Verde (Figure 5), with the model underestimating propane at every site by around a factor of 2. Similar to ethane, the largest absolute errors tend to be at the sites at higher latitudes such as Zeppelin and Pallas, where the RMSE exceed 400 ppt, however the NMB is similar at all sites, ranging from -52.7% at Zeppelin to -73.2% at Zugspitze.

https://doi.org/10.5194/egusphere-2023-2557
Preprint. Discussion started: 8 November 2023

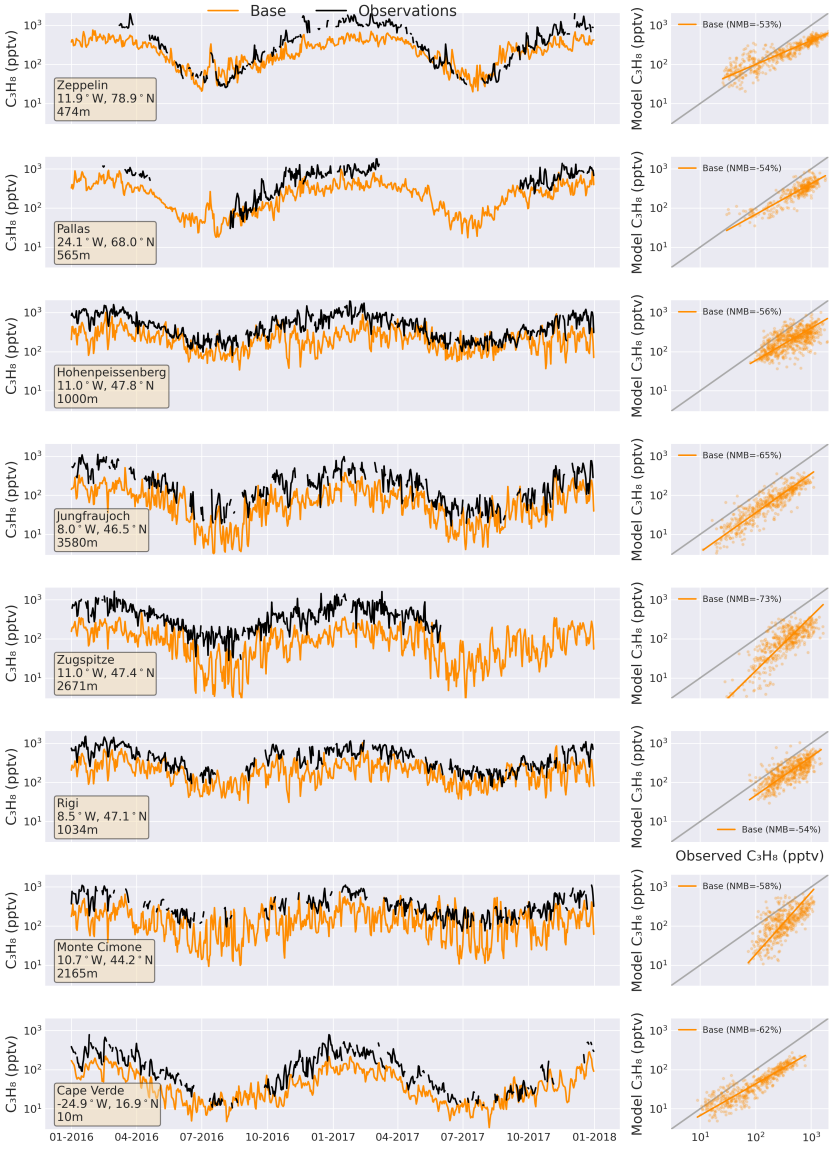

Figure 5. Observed (black line) daily mean concentrations of propane at 8 GAW sites compared with simulated concentrations using default CEDS emissions (orange).

The propane simulation is again consistent with previous work (Tzompa-Sosa et al., 2017; Dalsøren et al., 2018), and suggests an underestimate in the emissions of propane.

https://doi.org/10.5194/egusphere-2023-2557
Preprint. Discussion started: 8 November 2023

3.3 Higher alkanes

Model concentrations of the higher alkanes (ALK4 in GEOS-Chem) generally compare better to the observations than for ethane and propane (Figure 6), with an overall overestimate of 11.2%. The model generally underestimates higher alkanes at low concentrations, which may be exacerbated by the limit of detection in measured values of ∼1 ppt (WMO, 2021), meaning that the model can reach concentrations that are much lower than can be reliably measured. This is particularly noticeable in the Pacific Ocean, where the observed values at concentrations above 100 ppt generally compare well with the model, but there are large underestimates at concentrations below 100 ppt giving an overall RMSE of 187 ppt. Regionally, the model performs best over North America, with a NMB of 2.7%, while there are larger overestimates at sites in Europe and Asia (biases of 45.5% and 86.4%, respectively). Concentrations at Atlantic or Southern Hemispheric sites tend to be underestimated, with a small overall overestimate in the Pacific (4.7%), reflective of the model's tendency to underestimate higher alkanes where observed concentrations are low. Figure 7 shows the comparison between the simulated higher alkanes and those measured at 8 GAW sites. Across all sites there is an overestimate in modelled concentrations of 68.1%. Jungfraujoch, Zeppelin and Monte Cimone are the only sites with a negative bias, which is due to short peaks in measured concentrations which are not captured in the model, likely indicative of local pollution events. Whereas in periods without such peaks, such as winter at Zeppelin and early 2017 at Monte Cimone, concentrations are more often overestimated. The remaining sites see a consistent overestimate in concentrations, with the model performing worst at Pallas (NMB=192.5%) and best at Rigi (71.8%). The average model overestimate relative to the GAW sites is substantially greater than seen for the NOAA flask dataset (11.2%), however is similar in magnitude to the overestimate at European NOAA sites (45.5%). This may be the result of local and regional emissions being important at the GAW sites which are all European apart from Cape Verde, whereas many of the NOAA sites are very remote, marine or Southern Hemispheric where emissions are lower.

https://doi.org/10.5194/egusphere-2023-2557
Preprint. Discussion started: 8 November 2023

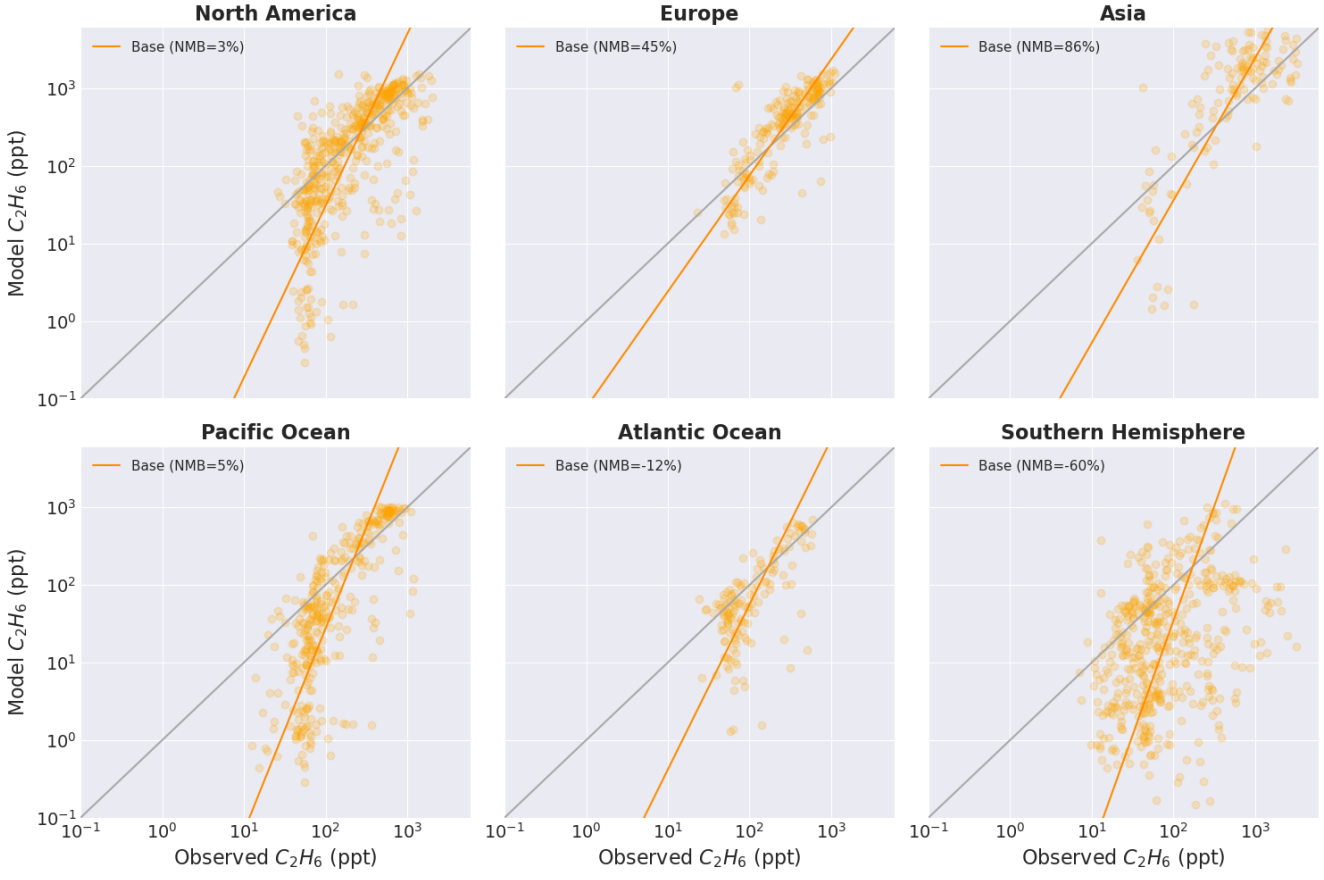

Figure 6. Modelled and observed hourly mean ALK4 concentrations in ppt. Simulated concentrations are compared to observed values for 43 NOAA Flask network sites for the years 2016-2017, split into 6 regions as labelled. An orthogonal distance regression (orange line) and 1 to 1 regression (grey) are also included.

https://doi.org/10.5194/egusphere-2023-2557
Preprint. Discussion started: 8 November 2023

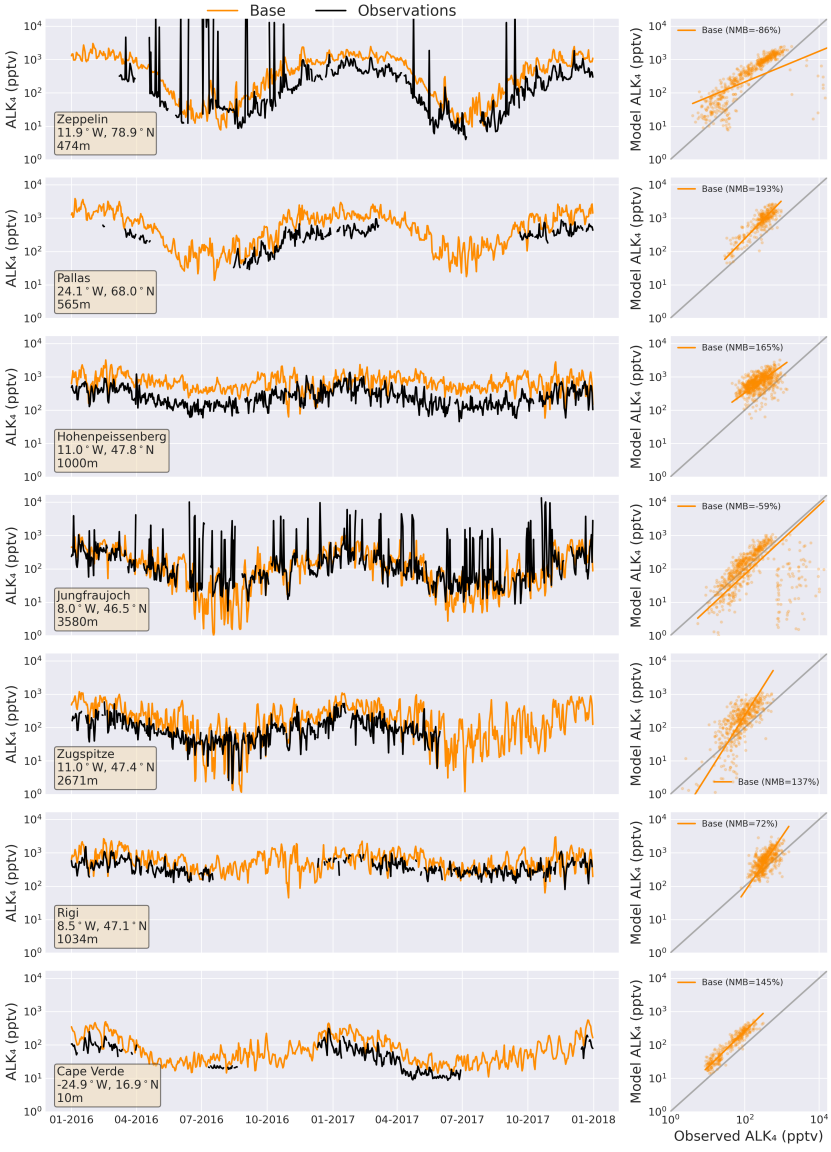

Figure 7. Observed (black line) daily mean concentrations of higher alkanes at 8 GAW sites compared with simulated concentrations using default CEDS emissions (orange).

3.3.1 Aromatic VOCs

As well as the alkanes we also examine the model performance simulating aromatic VOCs; benzene, toluene and xylene (Figure 8). Measurements of these compounds are less widespread, however there are a number of GAW sites in Europe as well as in Cape Verde, with data available for the period relevant to this study. For benzene, the model generally performs fairly well, with a low bias of -12.4%, and the line of best fit showing no clear systemic bias. For toluene and xylene, there is very high

https://doi.org/10.5194/egusphere-2023-2557
Preprint. Discussion started: 8 November 2023

variability in the comparison, resulting in larger underestimates in the model of -27.1% and -54.6% for toluene and xylene, respectively. Broadly, the model performs better overall for the aromatics than the alkanes, with relatively small underestimates across the available GAW sites, rather than the factor of two difference seen for simulated ethane and propane concentrations. However, there is little correlation between between the model and measurements for toluene or xylene.

https://doi.org/10.5194/egusphere-2023-2557
Preprint. Discussion started: 8 November 2023

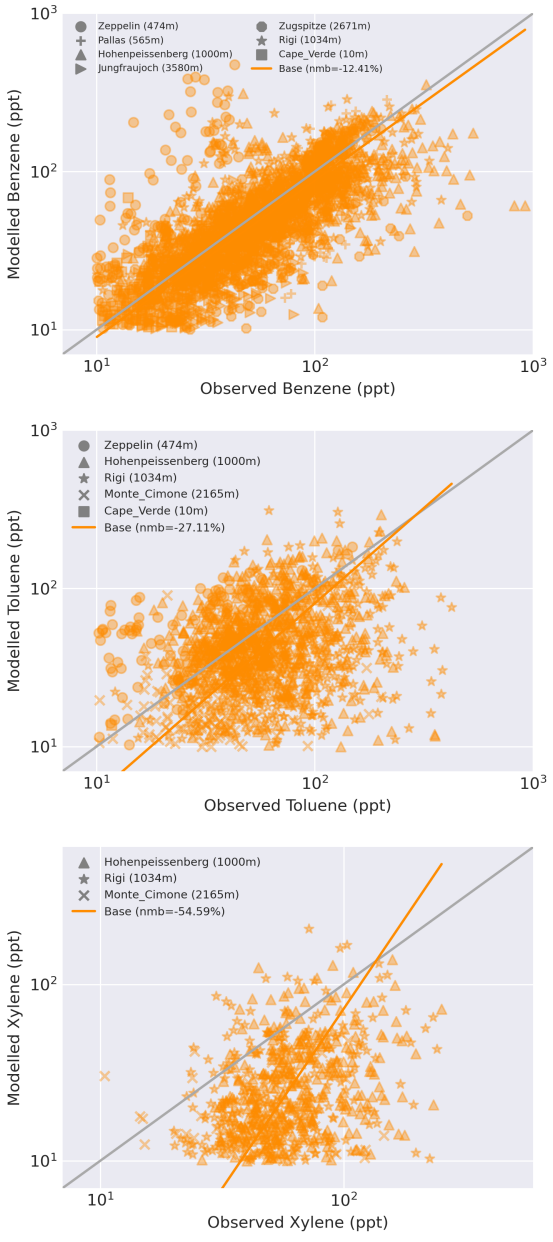

Figure 8. Modelled and observed hourly mean mixing ratios of aromatic VOCs benzene, toluene and xylene, in ppt. Simulated mixing ratios are compared to observed values from GAW sites in Europe and Cape Verde with data available for 2016-2017. An orthogonal distance regression (orange line) and 1 to 1 regression (grey) are also included.

https://doi.org/10.5194/egusphere-2023-2557
Preprint. Discussion started: 8 November 2023

Propene measurements from Cape Verde, Rigi and Hohenpeissenberg were also considered, however the model performs very poorly likely due to its short lifetime and a potential missing oceanic source which would be important in remote regions (Plass-Dülmer et al., 1993; Tripathi et al., 2020). Therefore propene isn't included further in this study.

3.3.2 Base Model Summary

The base simulation of ethane and propane appear consistent with previous work (Dalsøren et al., 2018; Emmons et al., 2015). The model underestimates concentrations by roughly a factor of two, beyond what could reasonably be expected through a model overestimate of the global tropospheric OH concentration. Naik et al. (2013) estimate OH concentration at 1.1 $\times 10^6$ molec cm^{-3} with an uncertainty of 7.0%. Even if the model OH concentration was shifted to the lower end of this range, it would not be sufficient extend the atmospheric lifetime enough to double the concentrations while maintaining the same emissions. Thus, given that there is no secondary chemical production of ethane or propane, we conclude that the current emissions of ethane and propane are underestimated.

The model simulation of higher alkanes (ALK4) overestimates the observations, which may be explained by the lumping of higher alkanes in GEOS-Chem, while using the OH rate constant associated with butane which is slower than that for pentanes and hexanes with large variability (Atkinson et al., 2006). For aromatic VOCs the observational network is less extensive but the model generally underestimates concentrations where measurements are available.

Given this we now explore whether using the NMVOC speciations found in regional emissions estimates will improve the model performance.

4 Regional anthropogenic NMVOC emissions

We now scale the CEDS total mass of NMVOC emissions in each gridbox by the mass speciation found in regional emissions estimates. Europe, the USA and China comprise 3 of the most important sources of anthropogenic NMVOC emissions, contributing approximately 60% of total global anthropogenic ethane emissions in the CEDS inventory.

The VOC speciation from a UK-based inventory is applied to all European VOC emissions, as the UK National Atmospheric Emissions Inventory (NAEI) provides highly speciated and detailed emissions, allowing precise translation to model NMVOC species. The NAEI is the UK's official inventory submitted under the National Emissions Ceilings Regulations (NECR) and Gothenburg Protocol to the United Nations Economic Commission for Europe Convention on Long-Range Transboundary Air Pollution (NAEI, 2023). The inventory covers over 400 individual sources of NMVOC, with a large contribution from a diverse range of industrial and agricultural processes, combustion and use of solvents, but with very few individually dominant sources. Further details on the methodology used to develop the NAEI and an explanation of emission trends are provided in the UK's annual Informative Inventory Report (NAEI, 2023) and in AQEG (2020). Emissions of individual NMVOC species are estimated using source-specific speciation profiles which show the mass fraction of each species, or in some cases groups of species, emitted by the source (AQEG, 2020; Passant, 2002). Over 600 individual NMVOC species or species groups are covered in the speciation, based on sources in industry, regulators and in some cases literature sources and databases such as

https://doi.org/10.5194/egusphere-2023-2557
Preprint. Discussion started: 8 November 2023

the USEPA SPECIATE database. The speciated inventory tends to be more uncertain than the inventory for total NMVOC and, whereas the inventory for total NMVOC is updated annually, the speciation profiles are only periodically updated when new information becomes available. Thus, trends in ethane and propane emissions for a sector shown by the NAEI are therefore a reflection of changes in total NMVOC emissions for the sector and do not normally reflect any changes over time in the speciation profile of the sector which may have occurred.

Speciated NMVOC emissions for the USA are from the US Environmental Protection Agency (EPA) distributed 2017 emissions modeling platform (2017 EMP). The 2017 EMP is derived from the 2017 National Emissions Inventories (US-EPA, 2021). The NEI is a synthesis of data gathered from state/local/tribal agencies and data directly produced at the EPA. Broadly, the NEI contains emissions data categorized by Source Classification Codes (SCC). The SCC data is provided for compound classes of pollutants (e.g., NO_x, VOC) at varying levels of spatial and temporal specificity. In the 2017 EMP, the NEI emissions from each SCC are spatially allocated to a model grid, temporally allocated to produce hour-specific rates, and speciated for a specific photochemical model configuration. For more details about the 2017 EMP, refer to the 2017 technical support document (US-EPA, 2022). The 2017 EMP data used here were provided as monthly totals (from hourly), on a 12 km lambert conformal grid, gases are speciated for CMAQ's Carbon Bond v6 revision 3 (CB6r3), and aerosols were speciated for CMAQ's aerosol module 7 (AE7). For use in GEOS-Chem, the 2017 EMP is translated for use with GEOS-Chem according to Lyssa and Henderson (doi: 10.5281/zenodo.5122827). To summarize, the 2017 EMP is remapped to a longitude latitude grid, vertical allocation is provided at high-level groupings of SCC, speciation is translated via HEMCO configuration, and hourly allocation is provided by HEMCO using the NEI99 inventory as a surrogate.

Speciated NMVOC emissions for China in 2017 are provided by the Multi-resolution Emission Inventory for China (MEIC) (Li et al., 2017a; Zheng et al., 2018). The MEIC inventory is based on a series of models and nationwide survey data, to estimate emissions of a range of gaseous and aerosol species in China (Li et al., 2017a). The MEIC provides several speciation methods for NMVOC emissions, here we use the SAPRC07 methodology (Carter, 2010; Li et al., 2014), as this includes the majority of the VOC species used in this study.

4.1 Re-speciating CEDS emissions using regional NMVOC emissions estimates

Figure 9 shows the NMVOC emissions speciation for Europe, USA and China for the 3 regional datasets compared to that from the CEDS global inventory. Ethane and propane emissions are considerably lower in the CEDS inventory for all 3 regions. The ratio of ethane emission to total NMVOC mass emissions is 0.02 over the USA in CEDS, compared to 0.12 in the EPA/NEI emissions. This results in USA ethane emissions in the NEI being around 6 times larger than in CEDS. Propane is similarly higher in each regional inventory compared to CEDS (Figure 9). This increase in ethane and propane is compensated for by lower ratios for the other VOC species, in particular the aromatics. Therefore, although the total NMVOC emissions in CEDS are almost identical to the totals in the regional inventories, they result in very different emissions of individual speciated VOCs. The substantially lower ethane and propane emissions in CEDS may explain the underestimate in simulated concentrations compared to observed values.

https://doi.org/10.5194/egusphere-2023-2557
Preprint. Discussion started: 8 November 2023

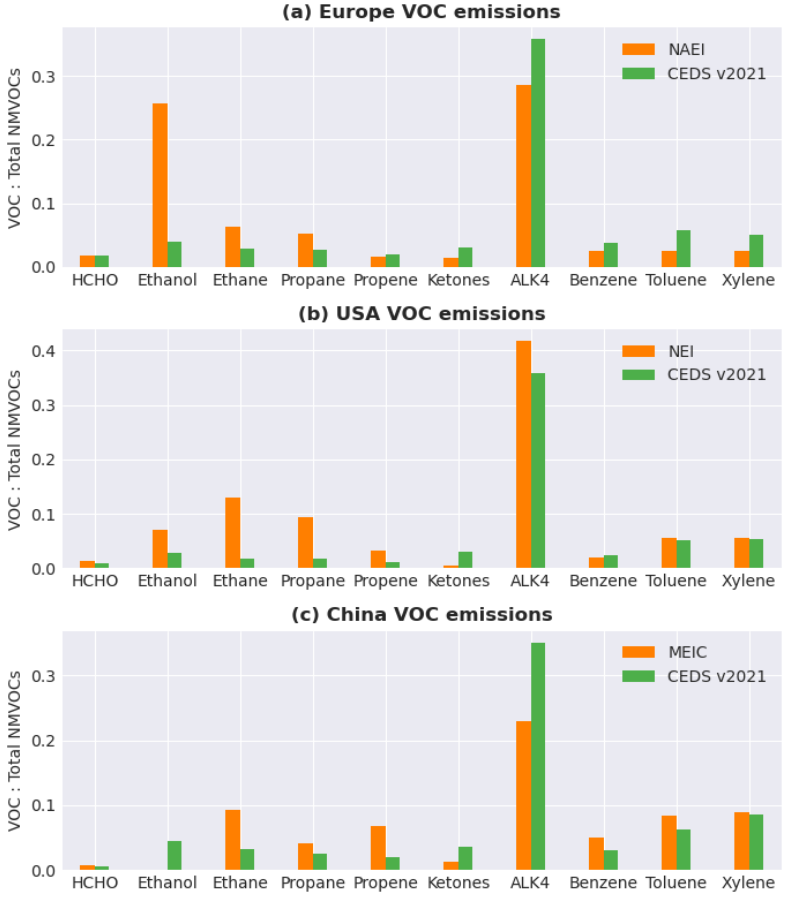

Figure 9. VOC mass emissions as fractional mass of total NMVOC emissions for Europe (top), USA (middle) and China (bottom). Regional emission estimates are in orange and the CEDS VOC emissions from the same regions are in green.

We apply the regional NMVOC speciations to the CEDS NMVOC emissions for each gridbox of the regions (USA, Europe and China). The re-speciation maintains the total NMVOC mass of emissions in each grid box, but adjusts the speciated NMVOC emission mass to the regional estimates for 2017, the most recent year with available emissions in all inventories. Emissions outside of these 3 regions are not changed, which notably includes India and the rest of Asia, Africa, and all of the Southern Hemisphere. Following the adjustment of regional CEDS emissions as described above, the model was run again for the same period to assess the effect of the re-speciated emissions.

https://doi.org/10.5194/egusphere-2023-2557
Preprint. Discussion started: 8 November 2023

5 Adjusted VOC emissions

5.1 Ethane

In Figure 10, simulated ethane using the re-speciated CEDS NMVOC emissions are compared with observations from the NOAA flask network together with the base model simulation. The model performance for ethane is substantially improved, increasing concentrations in all regions, particularly in the Northern Hemisphere where the re-speciation has been applied. The overall model bias has significantly reduced, from -35.0% to -3.8%, while the RMSE has roughly halved over North America, Europe and the Pacific and Atlantic Ocean sites. The largest improvement is seen at sites in North America and Europe where the bias has improved from -37.8% and -38.0%, to -3.6% and -4.1%, respectively, effectively removing the model low bias. Similar improvements are found over the Northern Hemispheric marine sites, despite the emissions remaining the same in those regions. Asia is the only region the modelled ethane hasn't improved, going from an underestimate of 18.7% to an overestimate of 26.0%, while the RMSE increases from 880 ppt to 933. This may indicate high uncertainty in VOC speciation in the regional database. Unsurprisingly, ethane concentrations in the Southern Hemisphere change the least in the new simulation, RMSE decreasing from 147 ppt to 139 ppt and NMB from -32.0% to -23.1%. As the re-speciation of anthropogenic emissions occurs entirely in the Northern Hemisphere this is as expected, with the atmospheric lifetime of ethane ($\sim$2 months (Helmig et al., 2014)) short enough to have only a small inter-hemispheric effect.

https://doi.org/10.5194/egusphere-2023-2557
Preprint. Discussion started: 8 November 2023

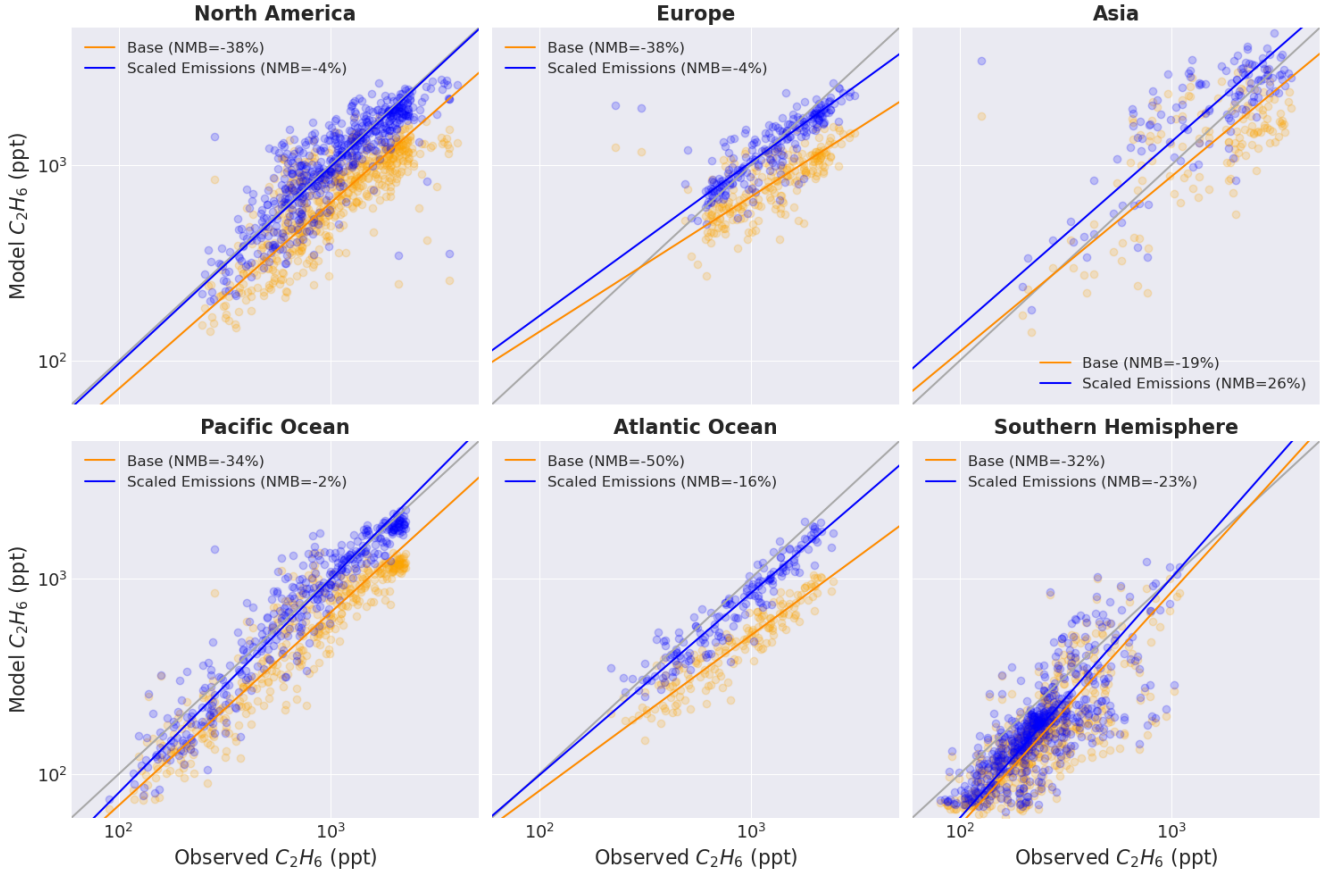

Figure 10. Modelled and observed ethane concentrations in ppt. Simulated concentrations using CEDS emissions (orange) and regionally scaled CEDS emissions (blue) are compared to observed values at 43 NOAA Flask network sites for the years 2016-2017, divided into 6 regions.

Figure 11 shows ethane concentrations from the re-speciated simulation against measurements from the GAW sites over the relevant period. As with the NOAA data, the model underestimate in ethane is decreased significantly, from -38.2% across the 7 sites to -5.7%. The improvement is consistent at all of the sites and throughout the measured period, approximately halving the RMSE at most sites and removing the systematic low-bias. At the Zeppelin Observatory and Rigi, Germany there
280 are now slight model overestimates (10.2% and 1.2%, respectively), while the other sites remain slightly underestimated, with Jungfraujoch having the largest remaining bias (-21.8%). Overall, the updated ethane simulations compare well with observed values throughout 2016-2017 at the GAW sites, and in all global regions with NOAA flask data. This suggests that the model's underestimate of ethane concentrations in the base simulation may be the result of the mechanism of NMVOC speciation, rather than errors in the total NMVOC emissions or the OH sink.

https://doi.org/10.5194/egusphere-2023-2557
Preprint. Discussion started: 8 November 2023

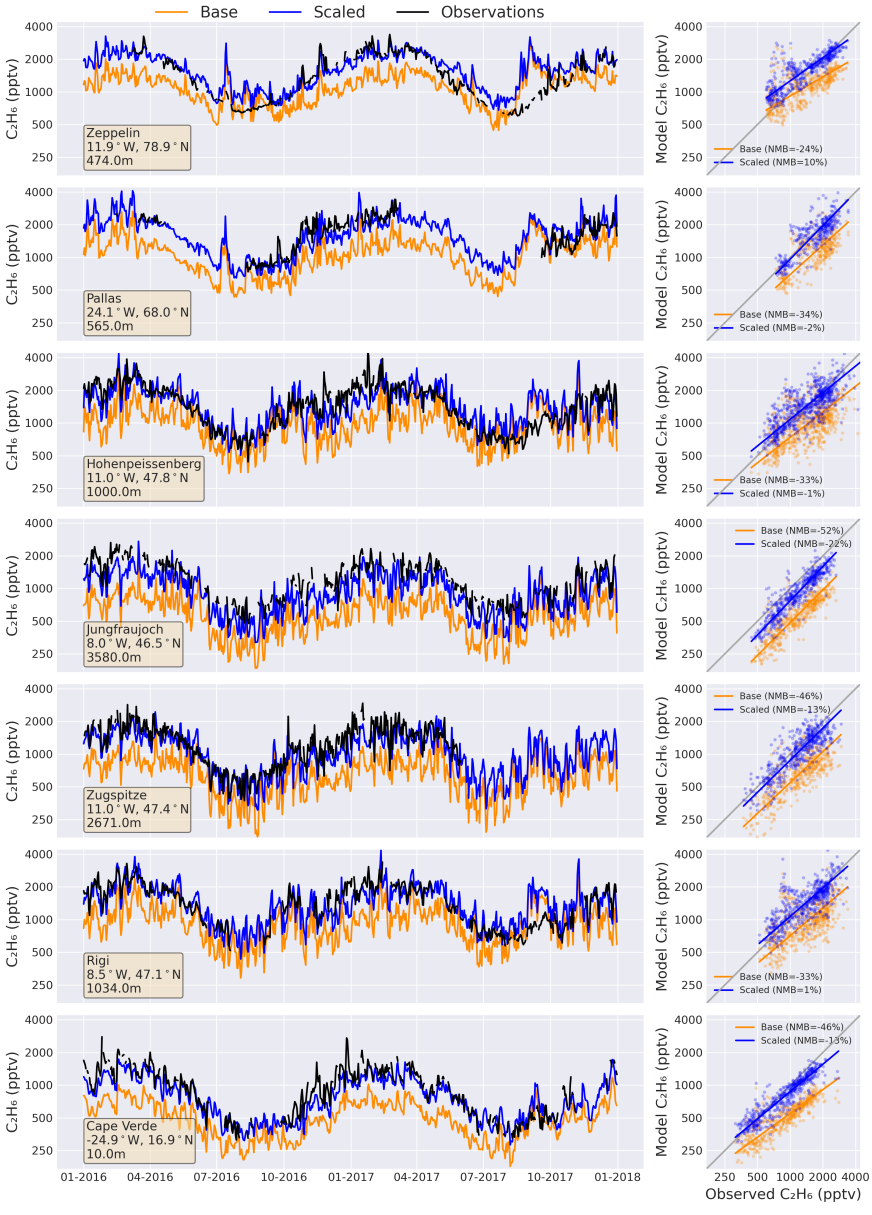

Figure 11. Observed (black line) daily mean concentrations of ethane at 7 GAW sites from 2016-2017, compared with the base GEOS-Chem simulation (orange) and the re-speciated CEDS emissions simulation (blue).

5.2 Propane

The re-speciation of the NMVOC emissions also results in improved model simulation of propane, with the bias compared to NOAA flask data improving from -63.8% to -48.0%. As with ethane, propane concentrations increase at almost every site

https://doi.org/10.5194/egusphere-2023-2557
Preprint. Discussion started: 8 November 2023

(Figure 12), as expected due to the increase in anthropogenic emissions of propane throughout the Northern Hemisphere. Over North America the RMSE decreases by ∼20% to 335 ppt, with the NMB improving from -63.7% to -44.6%. Similar improvements are seen across sites close to where the emissions have been changed in Asia and Europe, but unlike for ethane there remains an underestimate in the model concentrations in all of the 6 regions. Sites in the Atlantic in particular maintain a large underestimate with a NMB of -56.2% in the updated simulation, and a RMSE of 198 ppt. There is very little change in propane concentrations in the Southern Hemisphere due to the short atmospheric lifetime of propane (∼1 month (Rosado-Reyes and Francisco, 2007)), which limits hemispherical mixing but is long enough to allow Northern Hemisphere concentrations remote from emissions sources to increase.

Figure 13 shows the change in simulated propane concentrations relative to measurements from the 8 GAW sites. The overall picture is similar to Figure 12, with simulated propane concentrations increasing as a result of the re-speciation. This results in a decrease in the bias and error, although concentrations are still consistently underestimated by the model. The underestimate is smaller across all sites in the new simulation, with an overall NMB of -38.4%, from -59.2% in the base simulation. The highest altitude sites Jungfraujoch and Zugspitze-Schneefernerhaus have the largest underestimate in the re-speciated simulation, with NMBs of -42.6% and -56.9%, respectively. Unlike with ethane, there is no clear seasonality of the underestimate across the 8 sites, and while the new simulation increases concentrations, the slope of the line of best fit is approximately consistent with that in the base simulation at almost all sites. These results show that increasing anthropogenic propane emissions through the re-speciation of NMVOCs improves the model's ability to replicate propane concentrations globally. However, the remaining low model bias across all observations suggests that the re-speciation does not fully address the problem. It is possible that emissions outside of the 3 regions for which emissions were re-speciated are important for propane, and need to be included in the methodology to further improve modelled concentrations. In addition, there may be further propane sources currently missing from both global and regional emission inventories, resulting in an overall underestimate in propane and NMVOC emissions.

https://doi.org/10.5194/egusphere-2023-2557
Preprint. Discussion started: 8 November 2023

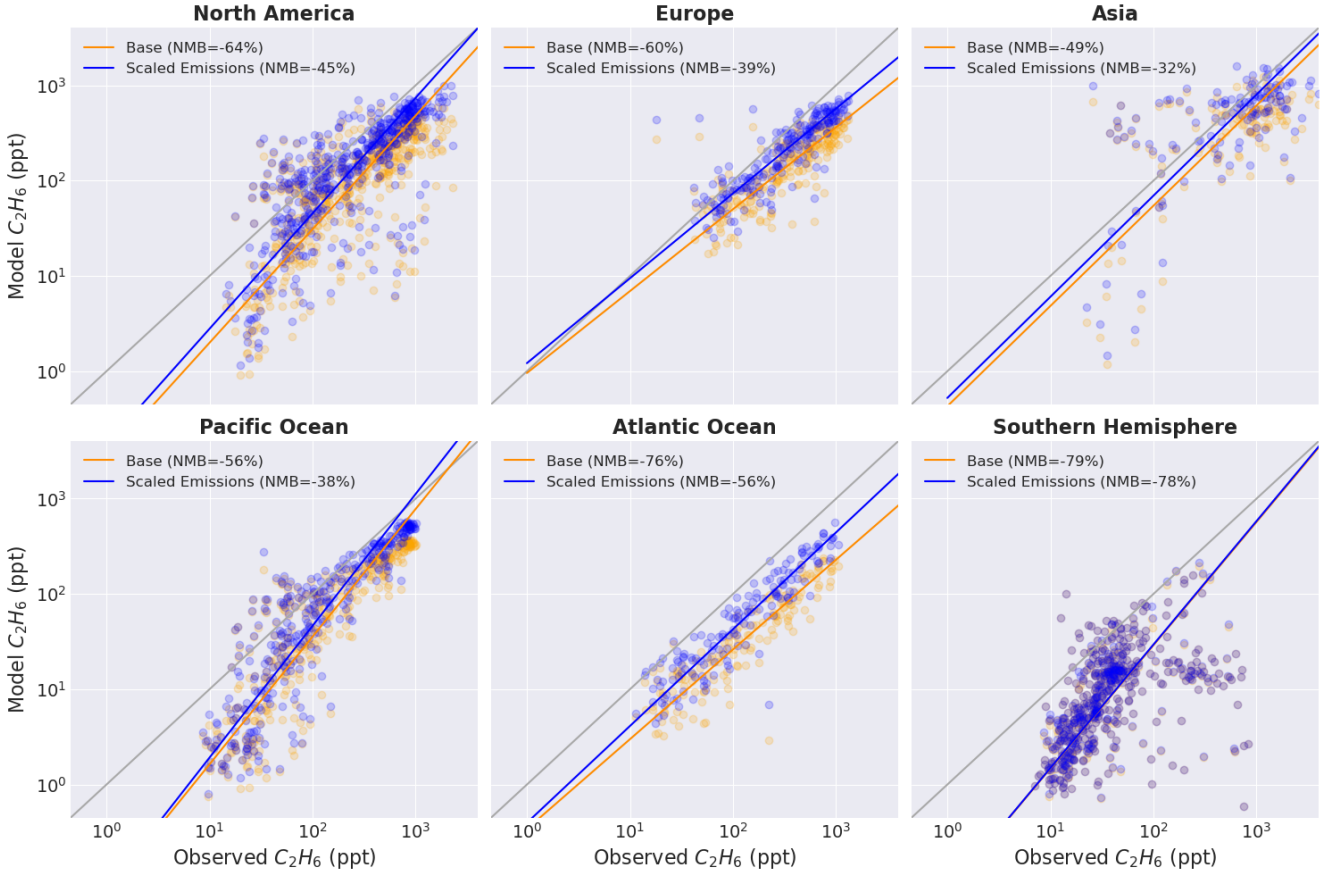

Figure 12. Modelled and observed propane concentrations in ppt. Simulated concentrations using CEDS emissions (orange) and regionally scaled CEDS emissions (blue) are compared to observed values at 43 NOAA Flask network sites for the years 2016-2017, divided into 6 regions.

https://doi.org/10.5194/egusphere-2023-2557
Preprint. Discussion started: 8 November 2023

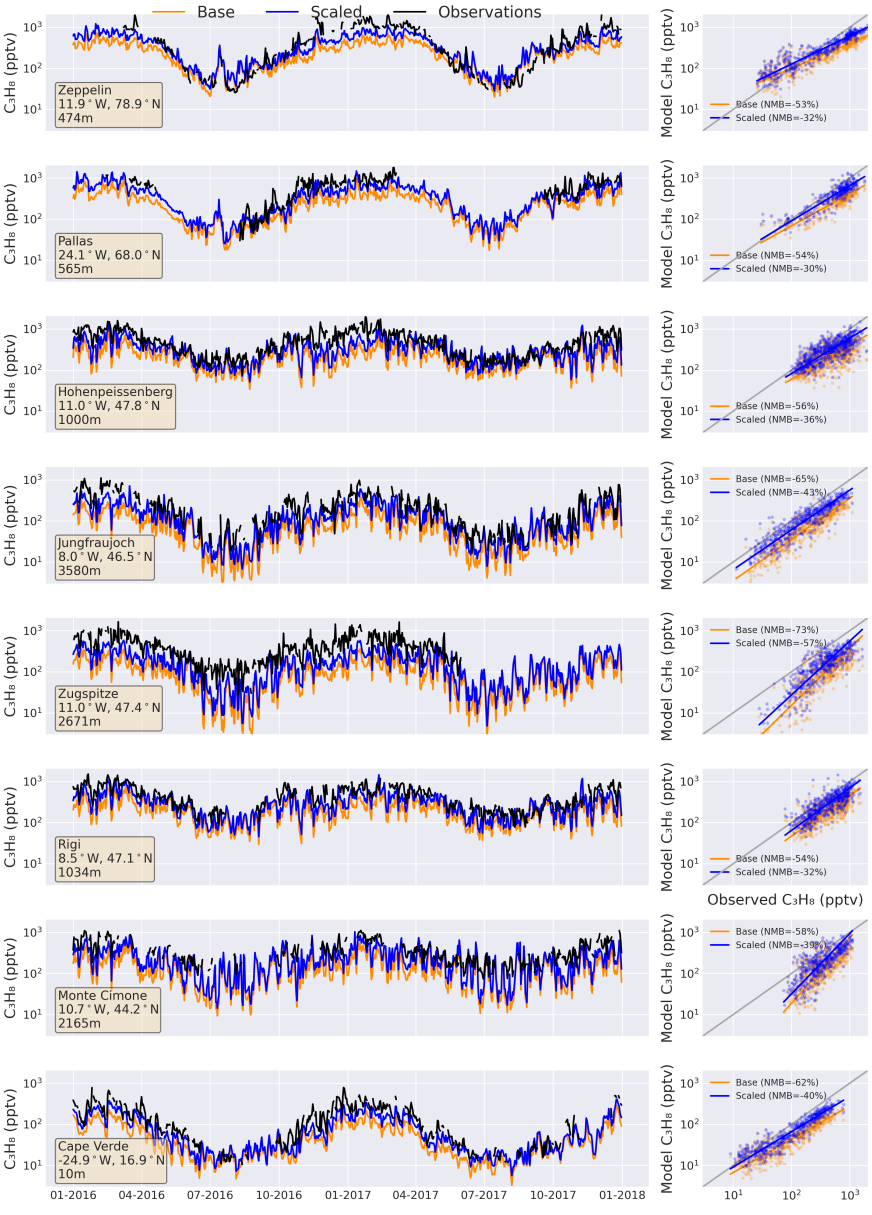

Figure 13. Observed (black line) daily mean concentrations of propane at 8 GAW sites from 2016-2017, compared with the base GEOS-Chem simulation (orange) and the re-speciated CEDS emissions simulation (blue).

5.3 Higher Alkanes

Changes to simulated higher alkane concentrations are smaller than those for ethane and propane (Figure 14), due to the smaller changes imposed during the re-speciation, and the contrast in the direction of the change in different regions; anthropogenic

https://doi.org/10.5194/egusphere-2023-2557
Preprint. Discussion started: 8 November 2023

emissions in North America increased, while decreasing in Europe and Asia (Figure 8). Comparing to the NOAA flask dataset (Figure 14), the re-speciated simulation removes the small overestimate in the simulated higher alkanes concentration, with the overall NMB changing from 11.2% to -1.4%. The largest improvements are found at European and Asian sites, where decreased emissions through the re-speciation result in lower concentrations of higher alkanes. NMB for European sites falls from 45.5% to 24.1%, while for Asia the change is 86.4% to 55.3%. Both regions therefore maintain a distinct overestimate in the model, however model performance is substantially improved with the new speciation. In contrast, model performance in marine regions gets worse, with the NMB going from 4.7% to -9.5% and -11.7% to -14.6% for Pacific and Atlantic sites, respectively. Over North America, the model bias changes from a small overestimate to a small underestimate (2.7% to -3.8%), despite a 16% increase in emissions of higher alkanes in the region. This is caused by larger decreases to emissions in other regions of the Northern Hemisphere (-20% in Europe, -34% in China), with the higher alkane atmospheric lifetime of approximately one week (Hodnebrog et al., 2018) sufficient to result in a small hemispheric impact. The change in the Southern Hemisphere however is negligible, as the lifetime is too short for inter-hemispheric mixing to occur. Figure 15 compares simulated higher alkane concentrations with 7 GAW sites across Europe and Cape Verde. NMB is decreased at 5 of the 7 sites, although changes in model performance tend to be small due to the relatively minor changes to total emissions. Simulated concentrations decrease at all sites, as expected following the decrease in higher alkane emissions from Europe and China. This results in an increased NMB at the Zepplin Observatory in Norway, however actually brings the model into better agreement with background concentrations.

https://doi.org/10.5194/egusphere-2023-2557
Preprint. Discussion started: 8 November 2023

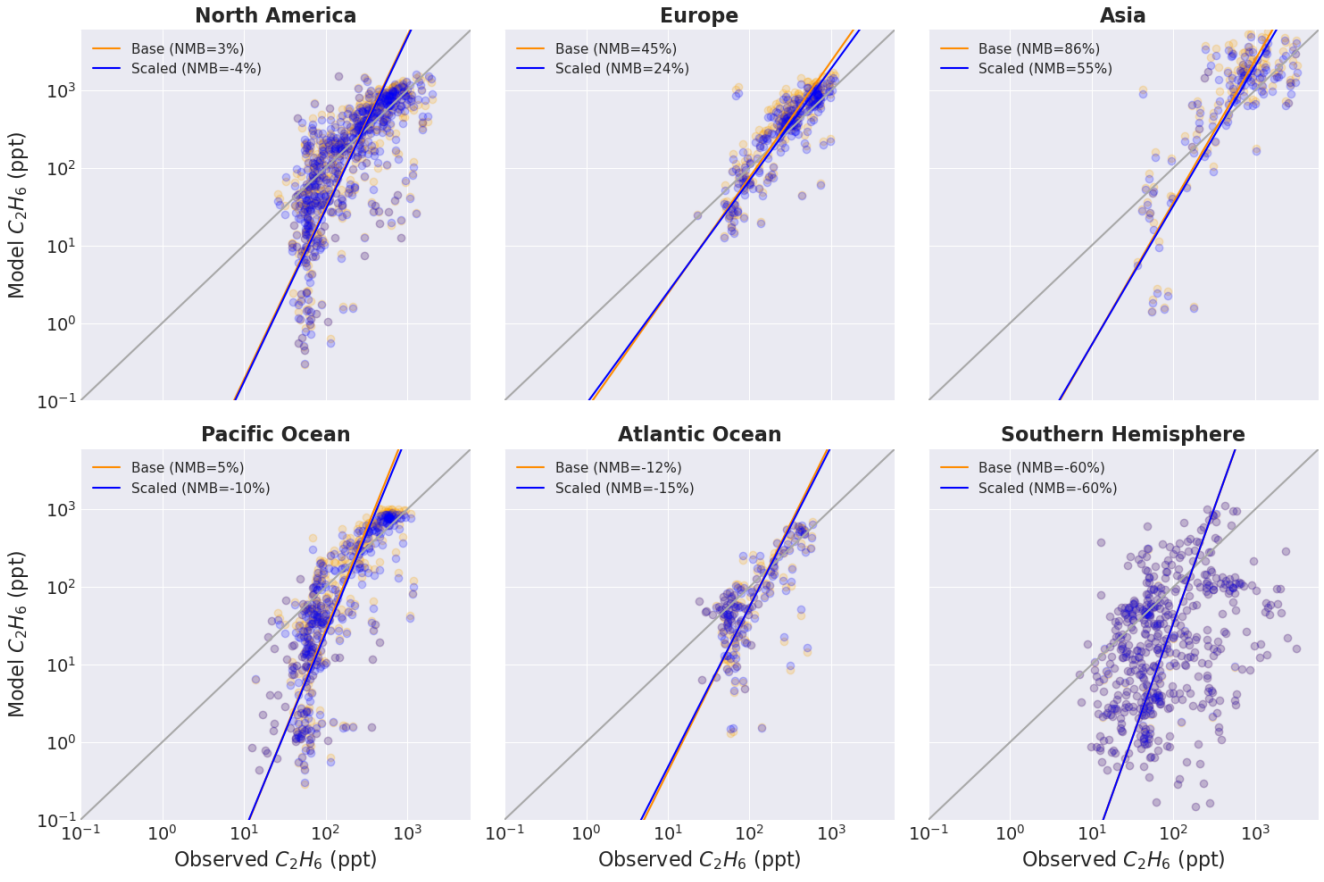

Figure 14. Modelled and observed ALK4 concentrations in ppt. Simulated concentrations using CEDS emissions (orange) and regionally scaled CEDS emissions (blue) are compared to observed values at 43 NOAA Flask network sites for the years 2016-2017, divided into 6 regions.

https://doi.org/10.5194/egusphere-2023-2557
Preprint. Discussion started: 8 November 2023

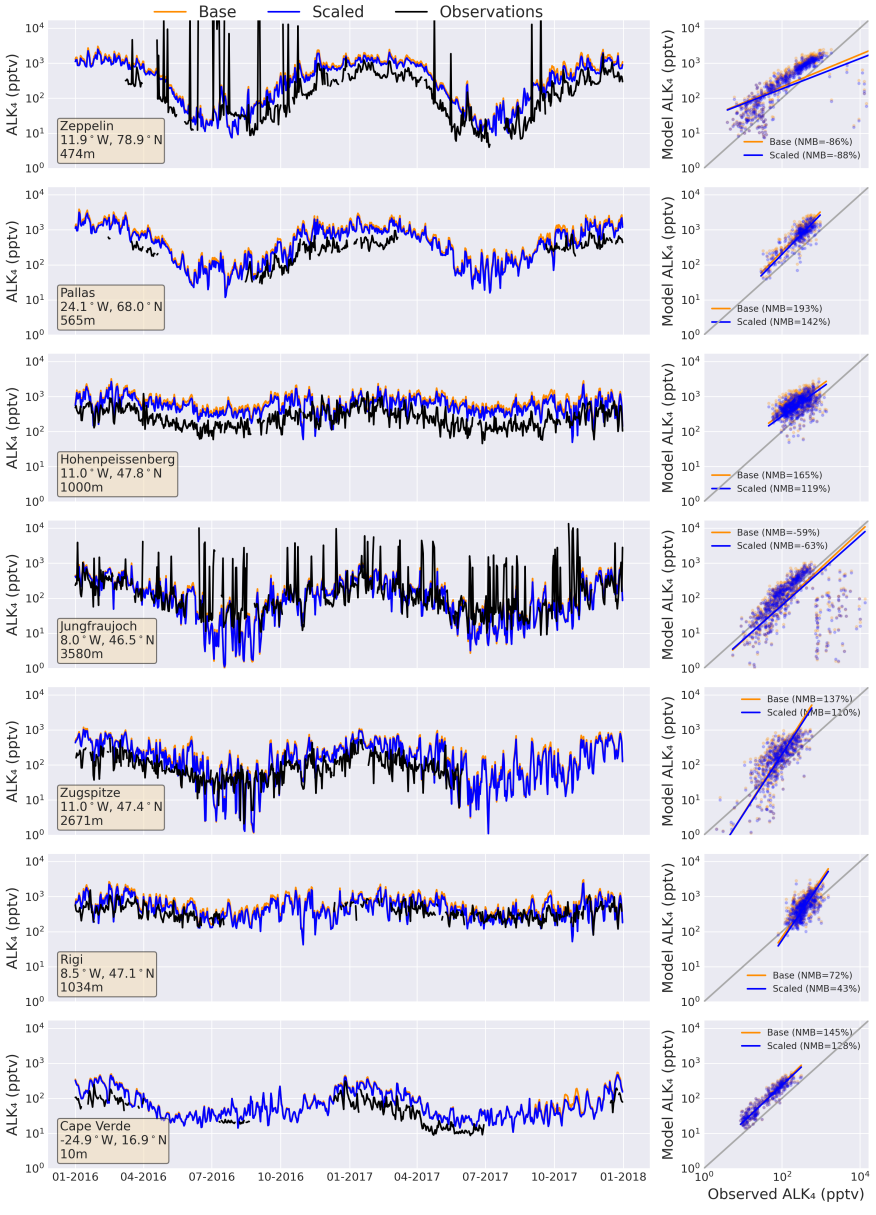

Figure 15. Observed (black line) daily mean concentrations of ALK4 at 7 GAW sites from 2016-2017, compared with the base GEOS-Chem simulation (orange) and the re-speciated CEDS emissions simulation (blue).

https://doi.org/10.5194/egusphere-2023-2557
Preprint. Discussion started: 8 November 2023

5.4 Aromatics

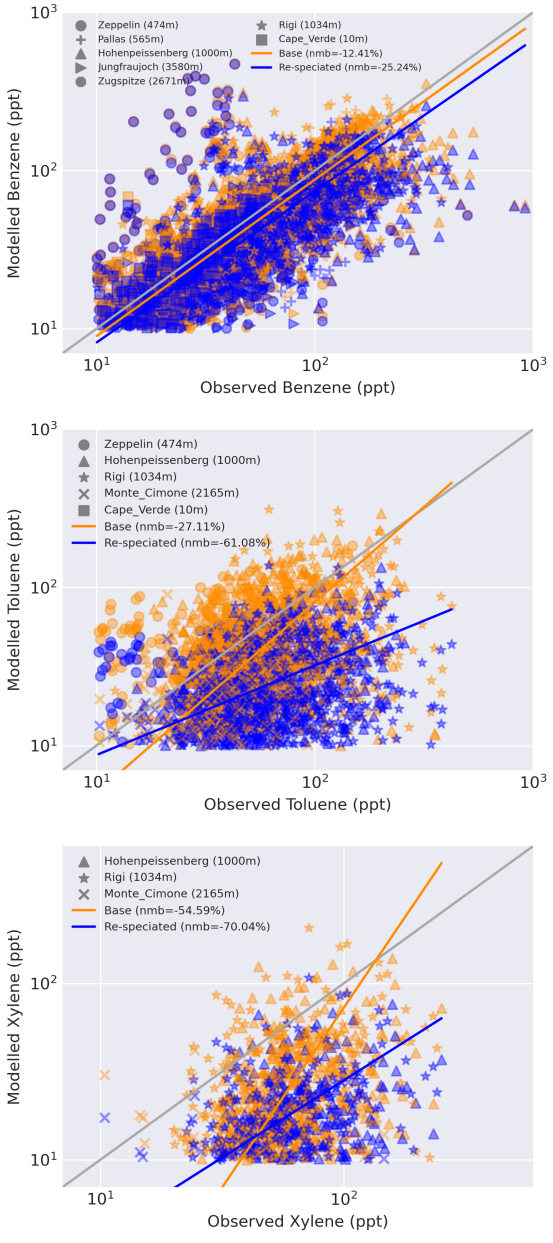

Figure 16. Modelled and observed hourly mean mixing ratios of aromatics VOCs benzene, toluene and xylene, in ppt. Simulated concentrations using CEDS emissions (orange) and re-speciated emissions (blue), are compared to observed values from GAW sites in Europe and Cape Verde with data available for 2016-2017. An orthogonal distance regression and 1 to 1 regression (grey) are also included.

https://doi.org/10.5194/egusphere-2023-2557
Preprint. Discussion started: 8 November 2023

The re-speciation of anthropogenic VOCs has a largely detrimental effect on the simulation of aromatics. All 3 species included here were underestimated in the base model simulation relative to WMO-GAW site data, and global emissions were decreased in the model during re-speciation, resulting in increased underestimation (Figure 16). For benzene and toluene this results in a doubling of the NMB, while for xylene the NMB also worsens, from -54.6% to -70.0%. The re-speciation methodology therefore does not result in uniform improvement across all NMVOCs. There may be missing aromatic emission sources which is resulting in a consistent underestimate, that cannot be rectified through improved NMVOC speciation.

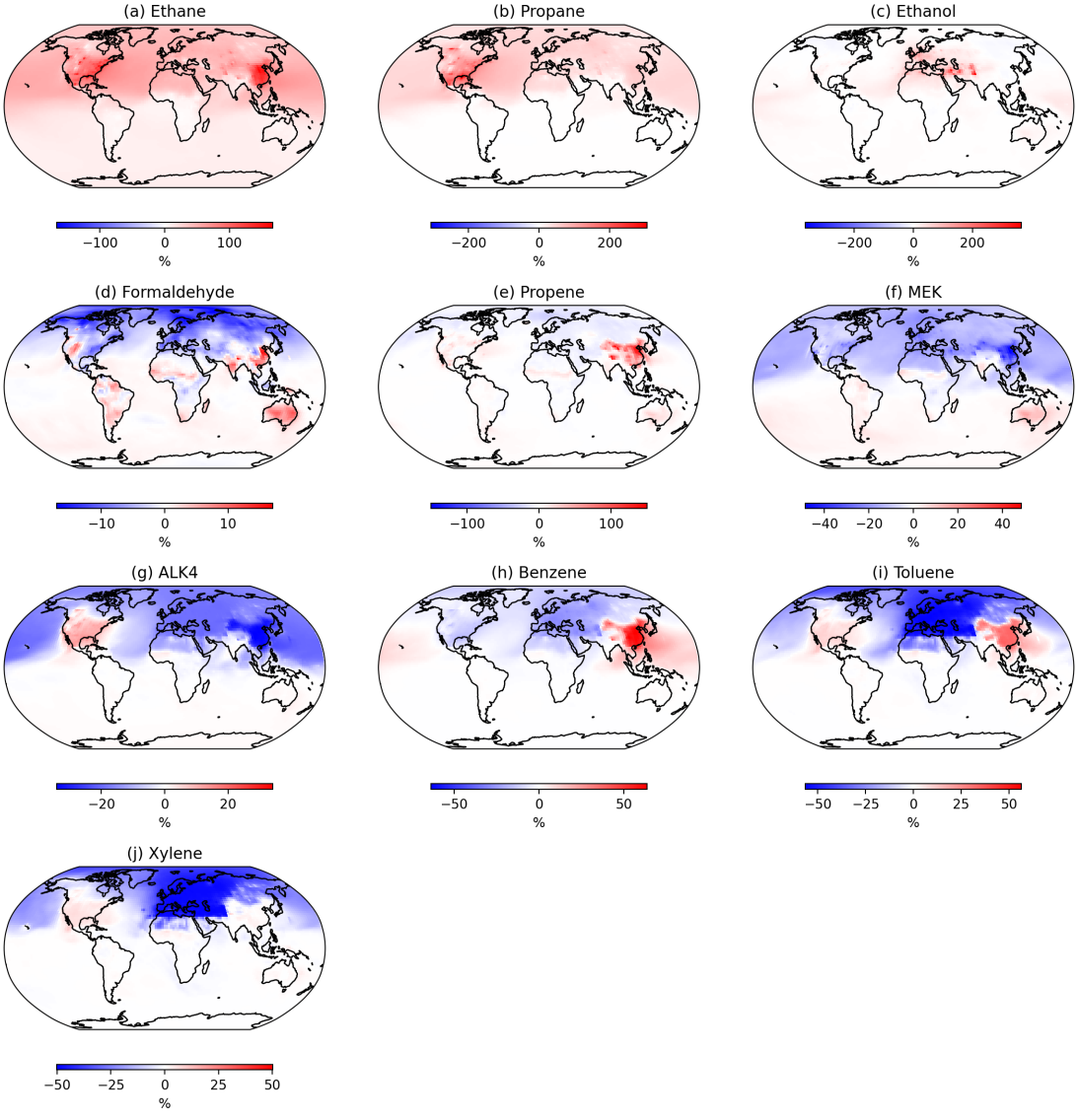

Figure 17. Simulated percentage change in annual mean surface concentrations of various VOC species.

https://doi.org/10.5194/egusphere-2023-2557
Preprint. Discussion started: 8 November 2023

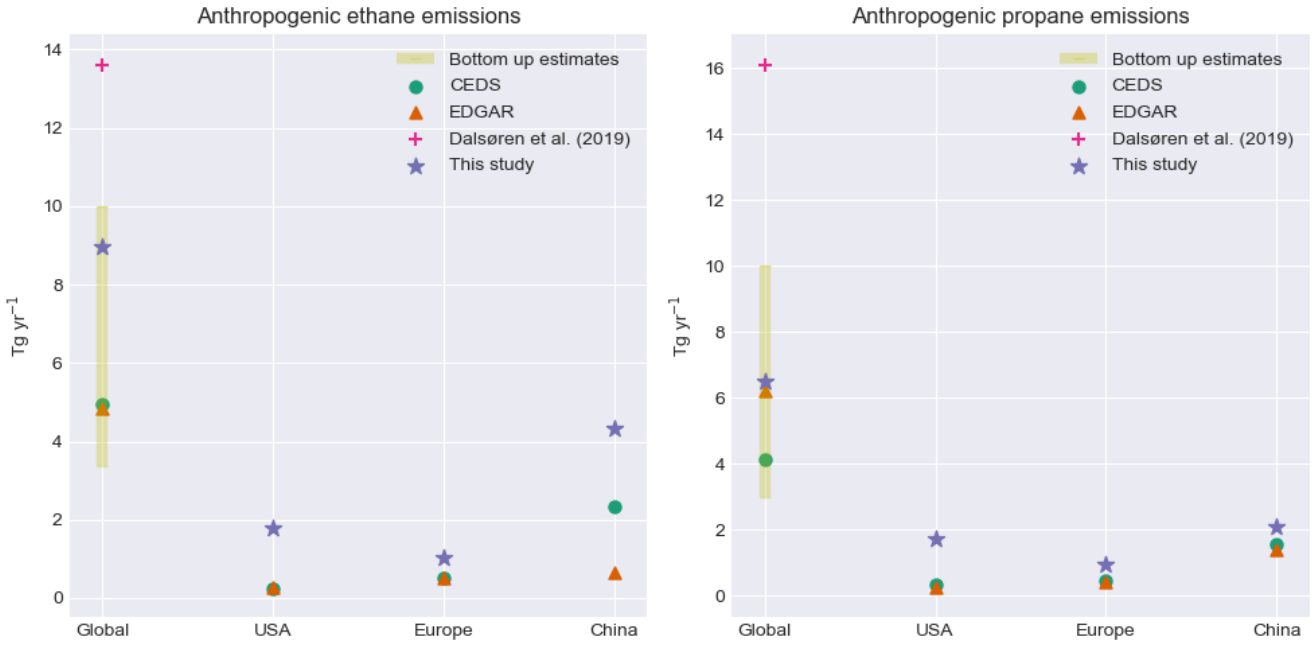

Figure 18. Annual anthropogenic emissions of ethane (left) and propane (right) globally and in key source regions, from global inventories (CEDS, EDGAR), a range of other bottom-up inventories Dalsøren et al. (2018) and this study following the re-speciation of CEDS emissions.

5.5 Discussion

The percentage change in the global annual mean surface concentrations of the re-speciated VOCs are shown in Figure 17. As expected, almost all of the changes in surface concentrations are restricted to the Northern Hemisphere, as the scale factors are only applied to emissions in this region. Increases in ethane and propane are largest in North America and China, where surface concentrations increased by more than 200%, and the global tropospheric burdens of ethane and propane increased by 17.2% and 33.9%, respectively. Concentrations throughout the Northern Hemisphere are roughly doubled compared to the base simulation, due to the relatively long atmospheric lifetimes of ethane and propane. Other VOCs predominantly change with the magnitude of the re-speciation in each region. Globally there is a decrease in the concentration of higher alkanes (ALK4) and aromatics (benzene, toluene and xylene), although with large regional variability. The scale of these changes is smaller than seen for ethane and propane, reflecting the smaller change to the emissions during re-speciation. Short-lived species such as ethanol, formaldehyde and propene have very localised impacts, while higher alkanes, ketones (MEK) and xylene lead to wider hemispheric impacts.

The changes in global and regional emissions of ethane and propane are shown in Figure 18. The re-speciation process increased global ethane emissions from those in CEDS by 4 Tg yr^{-1}, an increase of 81%, with the largest absolute increase in emissions over China, at 2 Tg yr^{-1}. The re-speciation resulted in a smaller increase in global propane emissions of 2.3 Tg yr^{-1}, a 57% increase on the CEDS inventory. Globally, the re-speciation results in a substantial increase in anthropogenic emissions

https://doi.org/10.5194/egusphere-2023-2557
Preprint. Discussion started: 8 November 2023

of both ethane and propane, but the total annual emissions remain comfortably within the range of the previous bottom-up studies. The increases are substantially lower than the optimized global total emissions estimated in Dalsøren et al. (2018). This may be a result of the OH concentration in those simulations being substantially higher than in GEOS-Chem (1.35×10^6 vs 1.06×10^6 molec cm^{-3}), resulting in a faster loss rate of VOCs and meaning that larger emissions are required to simulate observed concentrations. A simple OH correction of the Dalsoren study would suggest an emission of 10.6 Tg yr^{-1} for Ethane which is closer but slightly higher than the value of 9.9 Tg yr^{-1} used here (which doesn't included changes to emissions in India, Africa and the Southern Hemisphere). Given the differences in the OH concentrations we likely have some agreement on the ethane source. A similar correction for propane would give an emissions of 12.5 Tg yr^{-1} still substantially higher than those found here (6.5 Tg yr^{-1}), likely indicating that there is no agreement on the propane source.

5.6 Effect on atmospheric oxidation

In addition to directly influencing NMVOC concentrations, changes to NMVOC emissions can also influence atmospheric oxidation processes. Figure 19 shows the simulated change in global mean surface concentrations of tropospheric O_3 and OH, following the re-speciation of NMVOC emissions. Globally the changes are very small, with changes in annual mean surface O_3 and OH of 3.8% and -0.1%, respectively. The change in global tropospheric OH is similarly small (<1%), maintaining a mean annual concentration of 1.06×10^6 molec cm^{-3}. The tropospheric ozone burden increases from 313.3 Tg y^{-1} to 315.6 Tg yr^{-1}, an increase of just 0.7%. Regionally there are larger impacts, with increases in both O_3 and OH of ∼4-5% in East China, with a decrease of similar magnitude in OH over North America. However, despite large changes in relative concentrations of NMVOCs in the model, the changes to global atmospheric oxidation and tropospheric O_3 in particular are very small. There are several explanations for this, including the fact that the methodology maintains the same mass of emitted NMVOC, meaning that only differences in the relative reactivity of VOC species would affect the chemistry. Furthermore, the vast majority of the atmosphere is in a NOx-limited regime for O_3 production (Ivatt et al., 2022), thus, globally, changes in NMVOC concentrations are a relatively small lever on O_3 concentrations. This is supported by Edwards and Evans (2017), who showed that non-isoprene NMVOCs contribute in a very minor way to global tropospheric O_3 production, although can be important on regional scales.

https://doi.org/10.5194/egusphere-2023-2557
Preprint. Discussion started: 8 November 2023

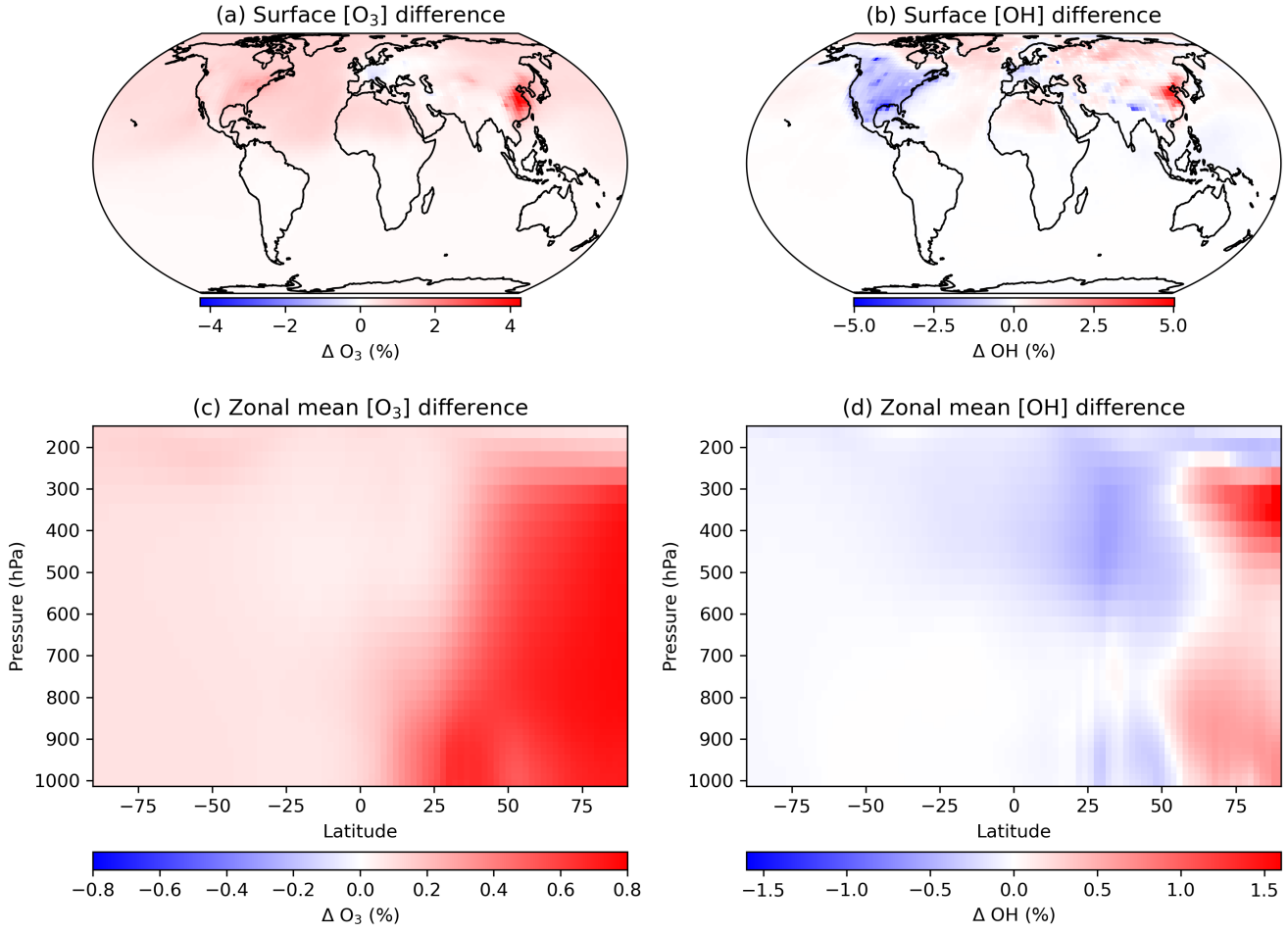

Figure 19. Top panels show the simulated percentage change in annual mean surface concentrations of O_3 (a) and OH (b). Lower panels show the annual mean percentage change through the troposphere for the same species.

6 Conclusions

Uncertainty in NMVOC speciation of anthropogenic emissions is large and at least partly responsible for poor model performance when simulating alkanes. We have shown that using regional NMVOC speciations rather than those used in CEDS significantly improves the simulation of ethane and propane concentrations in a global model. This effectively removes the underestimate in simulated ethane concentrations relative to observations. However, although modelled propane concentrations are improved, there remains a significant underestimate which might suggest a significant missing propane source. The

https://doi.org/10.5194/egusphere-2023-2557
Preprint. Discussion started: 8 November 2023

simulation of the higher alkanes is limited by the use of the OH rate constant consistent with butane, rather than all higher alkanes. Despite this the model performs well relative to observations of higher alkane concentrations, both before and after re-speciation. Simulated concentrations of aromatic species benzene, toluene and xylene generally degrade in the model following the re-speciation, resulting in a more marked increase in the underestimate compared to measured concentrations. This deterioration however is relatively small when compared to the improvement in the simulation of the alkanes. The improvement in the simulation of alkanes was achieved without altering the total NMVOCs emitted in the model and without detrimental impacts on the majority of other VOC species. The secondary impact on atmospheric oxidation is very small, due to the maintenance of total NMVOC emissions in the model, and the model being largely in a NOx-limited regime, resulting in minor changes to global tropospheric O_3 production.

Code and data availability. GEOS-Chem version 14.0.1 used in this study DOI: 10.5281/zenodo.7383492. Information and developments included in this version is available here http://wiki.seas.harvard.edu/geos-chem/index.php/GEOS-Chem_versions. Model output, observational datasets and processing code is archived at TBC. GAW datasets are available from the EBAR Archive (https://ebas-data.nilu.no/).

Author contributions. MJE and MJR developed the project. MJR performed the changes to emissions, ran the simulations and analysed the output. DH provided NOAA Flask observations and guidance. TM, NP and BR provided the description of the NAEI inventory and guidance for it's use. AL and LF provided processed version of the NAEI inventory for use in GEOS-Chem. LJC, KR and SP manage the CVAO site and data and provided the measurements used for evaluation. The paper was written by MJR with contributions from all co-authors

Competing interests. The authors declare that they have no conflict of interest.

Acknowledgements. This project was undertaken on the Viking Cluster, which is a high performance compute facility provided by the University of York. We are grateful for computational support from the University of York High Performance Computing service, Viking and the Research Computing team. We thank WMO GAW and the individual sites that make up this network, for the availability of the surface ozone data.

https://doi.org/10.5194/egusphere-2023-2557
Preprint. Discussion started: 8 November 2023

References

AQEG: Non-methane Volatile Organic Compounds in the UK. Report of the Air Quality Expert Group, Tech. rep., https://uk-air.defra.gov.uk/assets/documents/reports/cat09/2006240803_Non_Methane_Volatile_Organic_Compounds_in_the_UK.pdf, 2020.

Atkinson, R., Baulch, D. L., Cox, R. A., Crowley, J. N., Hampson, R. F., Hynes, R. G., Jenkin, M. E., Rossi, M. J., Troe, J., and Subcommittee, I.: Evaluated kinetic and photochemical data for atmospheric chemistry: Volume II; gas phase reactions of organic species, Atmospheric Chemistry and Physics, 6, 3625–4055, https://doi.org/10.5194/acp-6-3625-2006, 2006.

Aydin, M., Verhulst, K. R., Saltzman, E. S., Battle, M. O., Montzka, S. A., Blake, D. R., Qi Tang, Tang, Q., and Prather, M. J.: Recent decreases in fossil-fuel emissions of ethane and methane derived from firn air, Nature, 476, 198–201, https://doi.org/10.1038/nature10352, mAG ID: 2055535751, 2011.

Bates, K. H., Jacob, D. J., Li, K., Ivatt, P. D., Evans, M. J., Yan, Y., and Lin, J.: Development and evaluation of a new compact mechanism for aromatic oxidation in atmospheric models, Atmos. Chem. Phys., 21, 18 351–18 374, https://doi.org/10.5194/acp-21-18351-2021, 2021.

Bey, I., Jacob, D. J., Yantosca, R. M., Logan, J. A., Field, B. D., Fiore, A. M., Li, Q., Liu, H. Y., Mickley, L. J., and Schultz, M. G.: Global modeling of tropospheric chemistry with assimilated meteorology: Model description and evaluation, Journal of Geophysical Research: Atmospheres, 106, 23 073–23 095, https://doi.org/https://doi.org/10.1029/2001JD000807, 2001.

Boggs, P. T. and Donaldson, J. R.: Orthogonal Distance Regression, Applied and Computational Mathematics Division, nistir 89-4197, https://nvlpubs.nist.gov/nistpubs/Legacy/IR/nistir89-4197.pdf, 1989.

Carmichael, G. R., Tang, Y., Kurata, G., Uno, I., Streets, D. G., Thongboonchoo, N., Woo, J.-H., Guttikunda, S., White, A., Wang, T., Blake, D. R., Atlas, E., Fried, A., Potter, B., Avery, M. A., Sachse, G. W., Sandholm, S. T., Kondo, Y., Talbot, R. W., Bandy, A., Thorton, D., and Clarke, A. D.: Evaluating regional emission estimates using the TRACE-P observations, Journal of Geophysical Research: Atmospheres, 108, https://doi.org/https://doi.org/10.1029/2002JD003116, 2003.

Carpenter, L., Simpson, I., and Cooper, O.: Ground-Based Reactive Gas Observations Within the Global Atmosphere Watch (GAW) Network, pp. 1–21, Springer, Germany, https://doi.org/10.1007/978-981-15-2527-8_8-1, 2022.

Carter, W. P.: Development of the SAPRC-07 chemical mechanism, Atmospheric Environment, 44, 5324–5335, https://doi.org/https://doi.org/10.1016/j.atmosenv.2010.01.026, atmospheric Chemical Mechanisms: Selected Papers from the 2008 Conference, 2010.

Dalsøren, S. B., Myhre, G., Hodnebrog, O., Myhre, C. L., Stohl, A., Pisso, I., Schwietzke, S., Höglund-Isaksson, L., Helmig, D., Reimann, S., Sauvage, S., Schmidbauer, N., Read, K. A., Carpenter, L. J., Lewis, A. C., Punjabi, S., and Wallasch, M.: Discrepancy between simulated and observed ethane and propanelevels explained by underestimated fossil emissions, Nature Geoscience, 11, 178–184, https://doi.org/10.1038/s41561-018-0073-0, 2018.

Edwards, P. M. and Evans, M. J.: A new diagnostic for tropospheric ozone production, Atmos. Chem. Phys., 17, 13 669–13 680, https://doi.org/10.5194/acp-17-13669-2017, 2017.

EMEP/CEIP: Present state of emission data, https://www.ceip.at/webdab-emission-database/reported-emissiondataorhttps://www.ceip.at/status-of-reporting-and-review-results/2021-submissions, 2021.

Emmons, L. K., Arnold, S. R., Monks, S. A., Huijnen, V., Tilmes, S., Law, K. S., Thomas, J. L., Raut, J.-C., Bouarar, I., Turquety, S., Long, Y., Duncan, B., Steenrod, S., Strode, S., Flemming, J., Mao, J., Langner, J., Thompson, A. M., Tarasick, D., Apel, E. C., Blake, D. R., Cohen, R. C., Dibb, J., Diskin, G. S., Fried, A., Hall, S. R., Huey, L. G., Weinheimer, A. J., Wisthaler, A., Mikoviny, T., Nowak, J., Peischl,

https://doi.org/10.5194/egusphere-2023-2557
Preprint. Discussion started: 8 November 2023

J., Roberts, J. M., Ryerson, T., Warneke, C., and Helmig, D.: The POLARCAT Model Intercomparison Project (POLMIP): overview and evaluation with observations, Atmospheric Chemistry and Physics, 15, 6721–6744, https://doi.org/10.5194/acp-15-6721-2015, 2015.

Etiope, G. and Ciccioli, P.: Earth's Degassing: A Missing Ethane and Propane Source, Science, 323, 478–478, https://doi.org/10.1126/science.1165904, 2009.

Etiope, G., Ciotoli, G., Schwietzke, S., and Schoell, M.: Gridded maps of geological methane emissions and their isotopic signature, Earth System Science Data, 11, 1–22, https://doi.org/10.5194/essd-11-1-2019, 2019.

Franco, B., Mahieu, E., Emmons, L. K., Tzompa-Sosa, Z. A., Fischer, E. V., Sudo, K., Bovy, B., Conway, S., Griffin, D., Hannigan, J. W., Strong, K., and Walker, K. A.: Evaluating ethane and methane emissions associated with the development of oil and natural gas extraction in North America, Environmental Research Letters, 11, 044 010, https://doi.org/10.1088/1748-9326/11/4/044010, 2016.

Fry, M. M., Naik, V., West, J. J., Schwarzkopf, M. D., Fiore, A. M., Collins, W. J., Dentener, F. J., Shindell, D. T., Atherton, C., Bergmann, D., Duncan, B. N., Hess, P., MacKenzie, I. A., Marmer, E., Schultz, M. G., Szopa, S., Wild, O., and Zeng, G.: The influence of ozone precursor emissions from four world regions on tropospheric composition and radiative climate forcing, Journal of Geophysical Research: Atmospheres, 117, https://doi.org/https://doi.org/10.1029/2011JD017134, 2012.

Gelaro, R., McCarty, W., Suarez, M. J., Todling, R., Molod, A., Takacs, L., Randles, C. A., Darmenov, A., Bosilovich, M. G., Reichle, R., Wargan, K., Coy, L., Cullather, R., Draper, C., Akella, S., Buchard, V., Conaty, A., da Silva, A. M., Gu, W., Kim, G.-K., Koster, R., Lucchesi, R., Merkova, D., Nielsen, J. E., Partyka, G., Pawson, S., Putman, W., Rienecker, M., Schubert, S. D., Sienkiewicz, M., and Zhao, B.: The Modern-Era Retrospective Analysis for Research and Applications, Version 2 (MERRA-2), Journal of Climate, 30, 5419 – 5454, https://doi.org/10.1175/JCLI-D-16-0758.1, 2017.

Guenther, A., Hewitt, C. N., Erickson, D., Fall, R., Geron, C., Graedel, T., Harley, P., Klinger, L., Lerdau, M., Mckay, W. A., Pierce, T., Scholes, B., Steinbrecher, R., Tallamraju, R., Taylor, J., and Zimmerman, P.: A global model of natural volatile organic compound emissions, Journal of Geophysical Research: Atmospheres, 100, 8873–8892, https://doi.org/https://doi.org/10.1029/94JD02950, 1995.

Helmig, D., Petrenko, V. V., Martinerie, P., Witrant, E., Röckmann, T., Zuiderweg, A., Holzinger, R., Hueber, J., Thompson, C. R., Chelsea R. Thompson, White, J. W. C., Sturges, W. T., Baker, A. K., Blunier, T., Etheridge, D., Rubino, M., Tans, P. P., and Tans, P. P.: Reconstruction of Northern Hemisphere 1950–2010 atmospheric non-methane hydrocarbons, Atmospheric Chemistry and Physics, 14, 1463–1483, https://doi.org/10.5194/acp-14-1463-2014, mAG ID: 2133310200, 2014.

Helmig, D., Hueber, J., and Tans, P.: Flask-Air Sample Measurements of Atmospheric Non Methane Hydrocarbons Mole Fractions from the NOAA GML Carbon Cycle Surface Network at Global and Regional Background Sites, 2004-2016 (Version 2021.05.04) [Data set], University of Colorado Institute of Arctic and Alpine Research (INSTAAR). NOAA Global Monitoring Laboratory., https://doi.org/https://doi.org/10.15138/6AV8-GS57, 2021.

Hodnebrog, O., Dalsøren, S. B., and Myhre, G.: Lifetimes, direct and indirect radiative forcing, and global warming potentials of ethane (C2H6), propane (C3H8), and butane (C4H10), Atmospheric Science Letters, 19, e804, https://doi.org/10.1002/asl.804, 2018.

Hodzic, A., Kasibhatla, P. S., Jo, D. S., Cappa, C. D., Jimenez, J. L., Madronich, S., and Park, R. J.: Rethinking the global secondary organic aerosol (SOA) budget: stronger production, faster removal, shorter lifetime, Atmos. Chem. Phys., 16, 7917–7941, https://doi.org/10.5194/acp-16-7917-2016, 2016.

Hoesly, R. M., Smith, S. J., Feng, L., Klimont, Z., Janssens-Maenhout, G., Pitkanen, T., Seibert, J. J., Vu, L., Andres, R. J., Bolt, R. M., Bond, T. C., Dawidowski, L., Kholod, N., Kurokawa, J. I., Li, M., Liu, L., Lu, Z., Moura, M. C. P., O'Rourke, P. R., and Zhang, Q.: Historical (1750–2014) anthropogenic emissions of reactive gases and aerosols from the Community Emissions Data System (CEDS), Geosci. Model Dev., 11, 369–408, https://doi.org/10.5194/gmd-11-369-2018, 2018.

https://doi.org/10.5194/egusphere-2023-2557
Preprint. Discussion started: 8 November 2023

Ivatt, P. D., Evans, M. J., and Lewis, A. C.: Suppression of surface ozone by an aerosol-inhibited photochemical ozone regime, Nature Geoscience, 15, 536–540, https://www.nature.com/articles/s41561-022-00972-9, number: 7 Publisher: Nature Publishing Group, 2022.

Kirschke, S., Bousquet, P., Ciais, P., Saunois, M., Canadell, J. G., Dlugokencky, E. J., Bergamaschi, P., Bergmann, D., Blake, D. R., Bruhwiler, L., Cameron-Smith, P., Castaldi, S., Chevallier, F., Feng, L., Fraser, A., Heimann, M., Hodson, E. L., Houweling, S., Josse, B., Fraser, P. J., Krummel, P. B., Lamarque, J.-F., Langenfelds, R. L., Le Quéré, C., Naik, V., O'Doherty, S., Palmer, P. I., Pison, I., Plummer, D., Poulter, B., Prinn, R. G., Rigby, M., Ringeval, B., Santini, M., Schmidt, M., Shindell, D. T., Simpson, I. J., Spahni, R., Steele, L. P., Strode, S. A., Sudo, K., Szopa, S., van der Werf, G. R., Voulgarakis, A., van Weele, M., Weiss, R. F., Williams, J. E., and Zeng, G.: Three decades of global methane sources and sinks, Nature Geoscience, 6, 813–823, https://doi.org/10.1038/ngeo1955, 2013.

Koffi, B., Dentener, F., Janssens-Maenhout, G., Guizzardi, D., Crippa, M., Diehl, T., Galmarini, S., and Solazzo, E.: Hemispheric Transport of Air Pollution (HTAP): Specification of the HTAP2 experiments: Ensuring harmonized modelling, Tech. rep., Hemispheric Transport Air Pollution (HTAP), Luxembourg: Publications Office of the European Union, https://doi.org/10.2788/725244, 2016.

Li, M., Zhang, Q., Streets, D. G., He, K. B., Cheng, Y. F., Emmons, L. K., Huo, H., Kang, S. C., Lu, Z., Shao, M., Su, H., Yu, X., and Zhang, Y.: Mapping Asian anthropogenic emissions of non-methane volatile organic compounds to multiple chemical mechanisms, Atmospheric Chemistry and Physics, 14, 5617–5638, https://doi.org/10.5194/acp-14-5617-2014, 2014.

Li, M., Liu, H., Geng, G., Hong, C., Liu, F., Song, Y., Tong, D., Zheng, B., Cui, H., Man, H., Zhang, Q., and He, K.: Anthropogenic emission inventories in China: a review, National Science Review, 4, 834–866, https://doi.org/10.1093/nsr/nwx150, 2017a.

Li, M., Zhang, Q., Kurokawa, J. I., Woo, J. H., He, K., Lu, Z., Ohara, T., Song, Y., Streets, D. G., Carmichael, G. R., Cheng, Y., Hong, C., Huo, H., Jiang, X., Kang, S., Liu, F., Su, H., and Zheng, B.: MIX: a mosaic Asian anthropogenic emission inventory under the international collaboration framework of the MICS-Asia and HTAP, Atmos. Chem. Phys., 17, 935–963, https://doi.org/10.5194/acp-17-935-2017, 2017b.

McDuffie, E. E., Smith, S. J., O'Rourke, P., Tibrewal, K., Venkataraman, C., Marais, E. A., Zheng, B., Crippa, M., Brauer, M., and Martin, R. V.: A global anthropogenic emission inventory of atmospheric pollutants from sector- and fuel-specific sources (1970–2017): an application of the Community Emissions Data System (CEDS), Earth System Science Data, 12, 3413–3442, https://essd.copernicus.org/articles/12/3413/2020/, publisher: Copernicus GmbH, 2020.

Monks, P. S., Archibald, A. T., Colette, A., Cooper, O., Coyle, M., Derwent, R., Fowler, D., Granier, C., Law, K. S., Mills, G. E., Stevenson, D. S., Tarasova, O., Thouret, V., von Schneidemesser, E., Sommariva, R., Wild, O., and Williams, M. L.: Tropospheric ozone and its precursors from the urban to the global scale from air quality to short-lived climate forcer, Atmos. Chem. Phys., 15, 8889–8973, https://doi.org/10.5194/acp-15-8889-2015, 2015.

NAEI: UK Informative Inventory Report (1990 to 2021)., Tech. rep., https://uk-air.defra.gov.uk/assets/documents/reports/cat09/2303151609_UK_IIR_2023_Submission.pdf, 2023.

Naik, V., Voulgarakis, A., Fiore, A. M., Horowitz, L. W., Lamarque, J.-F., Lin, M., Prather, M. J., Young, P. J., Bergmann, D., Cameron-Smith, P. J., Cionni, I., Collins, W. J., Dalsøren, S. B., Doherty, R., Eyring, V., Faluvegi, G., Folberth, G. A., Josse, B., Lee, Y. H., MacKenzie, I. A., Nagashima, T., van Noije, T. P. C., Plummer, D. A., Righi, M., Rumbold, S. T., Skeie, R., Shindell, D. T., Stevenson, D. S., Strode, S., Sudo, K., Szopa, S., and Zeng, G.: Preindustrial to present-day changes in tropospheric hydroxyl radical and methane lifetime from the Atmospheric Chemistry and Climate Model Intercomparison Project (ACCMIP), Atmospheric Chemistry and Physics, 13, 5277–5298, https://doi.org/10.5194/acp-13-5277-2013, publisher: Copernicus GmbH, 2013.

https://doi.org/10.5194/egusphere-2023-2557
Preprint. Discussion started: 8 November 2023

Nicewonger, M. R., Verhulst, K. R., Aydin, M., and Saltzman, E. S.: Preindustrial atmospheric ethane levels inferred from polar ice cores: A constraint on the geologic sources of atmospheric ethane and methane, Geophysical Research Letters, 43, 214–221, https://doi.org/https://doi.org/10.1002/2015GL066854, 2016.

Passant, N. R.: Speciation of UK emissions of non-methane volatile organic compounds. NAEI Report AEAT/ENV/R/0545 prepared for DETR Air and Environmental Quality Division, Tech. rep., https://uk-air.defra.gov.uk/assets/documents/reports/empire/AEAT_ENV_0545_final_v2.pdf, 2002.

Plass-Dülmer, C., Khedim, A., Koppmann, R., Johnen, F. J., Rudolph, J., and Kuosa, H.: Emissions of light nonmethane hydrocarbons from the Atlantic into the atmosphere, Global Biogeochemical Cycles, 7, 211–228, https://onlinelibrary.wiley.com/doi/abs/10.1029/92GB02361, _eprint: https://onlinelibrary.wiley.com/doi/pdf/10.1029/92GB02361, 1993.

Pozzer, A., Jöckel, P., Tost, H., Sander, R., Ganzeveld, L., Ganzeveld, L., Kerkweg, A., Kerkweg, A., and Lelieveld, J.: Simulating organic species with the global atmospheric chemistry general circulation model ECHAM5/MESSy1: a comparison of model results with observations, Atmospheric Chemistry and Physics, 7, 2527–2550, https://doi.org/10.5194/acp-7-2527-2007, mAG ID: 2117453089, 2007.

Pozzer, A., Pollmann, J., Taraborrelli, D., Jöckel, P., Helmig, D., Tans, P. P., Tans, P. P., Hueber, J., and Lelieveld, J.: Observed and simulated global distribution and budget of atmospheric C 2 -C 5 alkanes, Atmospheric Chemistry and Physics, 10, 4403–4422, https://doi.org/10.5194/acp-10-4403-2010, mAG ID: 2048846813, 2010.

Prather, M. J., Holmes, C. D., and Hsu, J.: Reactive greenhouse gas scenarios: Systematic exploration of uncertainties and the role of atmospheric chemistry, Geophysical Research Letters, 39, https://doi.org/https://doi.org/10.1029/2012GL051440, 2012.

Rosado-Reyes, C. M. and Francisco, J. S.: Atmospheric oxidation pathways of propane and its by-products: Acetone, acetaldehyde, and propionaldehyde, Journal of Geophysical Research: Atmospheres, 112, https://doi.org/https://doi.org/10.1029/2006JD007566, 2007.

Simpson, D., Winiwarter, W., Börjesson, G., Cinderby, S., Ferreiro, A., Guenther, A., Hewitt, C. N., Janson, R., Khalil, M. A. K., Owen, S., Pierce, T. E., Puxbaum, H., Shearer, M., Skiba, U., Steinbrecher, R., Tarrasón, L., and Öquist, M. G.: Inventorying emissions from nature in Europe, Journal of Geophysical Research: Atmospheres, 104, 8113–8152, https://doi.org/https://doi.org/10.1029/98JD02747, 1999.

Simpson, I. J., Andersen, M. P. S., Meinardi, S., Bruhwiler, L., Blake, N. J., Helmig, D., Rowland, F. S., and Blake, D. R.: Long-term decline of global atmospheric ethane concentrations and implications for methane, Nature, 488, 490–494, https://doi.org/10.1038/nature11342, mAG ID: 2071148466, 2012.

Szopa, S., Naik, V., Adhikary, B., Artaxo, P., Berntsen, T., Collins, W., Fuzzi, S., Gallardo, L., Kiendler-Scharr, A., Klimont, Z., Liao, H., Unger, N., and Zanis, P.: Short-Lived Climate Forcers, p. 817–922, Cambridge University Press, Cambridge, United Kingdom and New York, NY, USA, https://doi.org/10.1017/9781009157896.008, 2021a.

Szopa, S., Naik, V., Adhikary, B., Artaxo, P., Berntsen, T., Collins, W., Fuzzi, S., Gallardo, L., Kiendler-Scharr, A., Klimont, Z., Liao, H., Unger, N., and Zanis, P.: Short-Lived Climate Forcers. In Climate Change 2021: The Physical Science Basis. Contribution of Working Group I to the Sixth Assessment Report of the Intergovernmental Panel on Climate Change, Report, IPCC, https://doi.org/doi:10.1017/9781009157896.008, 2021b.

Tripathi, N., Sahu, L. K., Singh, A., Yadav, R., Patel, A., Patel, K., and Meenu, P.: Elevated Levels of Biogenic Non-methane Hydrocarbons in the Marine Boundary Layer of the Arabian Sea During the Intermonsoon, Journal of Geophysical Research: Atmospheres, 125, e2020JD032 869, https://onlinelibrary.wiley.com/doi/abs/10.1029/2020JD032869, _eprint: https://onlinelibrary.wiley.com/doi/pdf/10.1029/2020JD032869, 2020.

Tzompa-Sosa, Z. A., Mahieu, E., Franco, B., Keller, C. A., Turner, A. J., Helmig, D., Fried, A., Richter, D., Weibring, P., Walega, J., Yacovitch, T. I., Herndon, S. C., Blake, D. R., Hase, F., Hannigan, J. W., Conway, S., Strong, K., Schneider, M., and Fischer,

https://doi.org/10.5194/egusphere-2023-2557
Preprint. Discussion started: 8 November 2023

E. V.: Revisiting global fossil fuel and biofuel emissions of ethane, Journal of Geophysical Research: Atmospheres, 122, 2493–2512, https://doi.org/https://doi.org/10.1002/2016JD025767, 2017.

US-EPA: 2017 National Emissions Inventory: January 2021 Updated Release, Technical Support Document, U.S. Environmental Protection Agency, https://www.epa.gov/air-emissions-inventories/2017-national-emissions-inventory-nei-technical-support-document-tsd, 2021.

US-EPA: Preparation of Emissions Inventories for the 2017 North American Emissions Modeling Platform (Technical Support Document EPA-454/B-22-002), U.S. Environmental Protection Agency, https://www.epa.gov/air-emissions-modeling/2017-emissions-modeling-platform-technical-support-document, 2022.

van der Werf, G. R., Randerson, J. T., Giglio, L., van Leeuwen, T. T., Chen, Y., Rogers, B. M., Mu, M., van Marle, M. J. E., Morton, D. C., Collatz, G. J., Yokelson, R. J., and Kasibhatla, P. S.: Global fire emissions estimates during 1997–2016, Earth System Science Data, 9, 697–720, https://doi.org/10.5194/essd-9-697-2017, 2017.

Voulgarakis, A., Naik, V., Lamarque, J.-F., Shindell, D. T., Young, P. J., Prather, M. J., Wild, O., Field, R. D., Bergmann, D., Cameron-Smith, P., Cionni, I., Collins, W. J., Dalsøren, S. B., Doherty, R. M., Eyring, V., Faluvegi, G., Folberth, G. A., Horowitz, L. W., Josse, B., MacKenzie, I. A., Nagashima, T., Plummer, D. A., Righi, M., Rumbold, S. T., Stevenson, D. S., Strode, S. A., Sudo, K., Szopa, S., and Zeng, G.: Analysis of present day and future OH and methane lifetime in the ACCMIP simulations, Atmospheric Chemistry and Physics, 13, 2563–2587, https://doi.org/10.5194/acp-13-2563-2013, 2013.

WMO: GAW Report no. 265: System and Performance audit for Non-Methane Volatile Organic Compounds at the Global GAW Station Cape Verde, December 2019, https://library.wmo.int/doc_num.php?explnum_id=10725, 2021.

Xiao, Y., Logan, J. A., Jacob, D. J., Hudman, R. C., Yantosca, R., and Blake, D. R.: Global budget of ethane and regional constraints on U.S. sources, Journal of Geophysical Research: Atmospheres, 113, https://doi.org/https://doi.org/10.1029/2007JD009415, 2008.

Zheng, B., Tong, D., Li, M., Liu, F., Hong, C., Geng, G., Li, H., Li, X., Peng, L., Qi, J., Yan, L., Zhang, Y., Zhao, H., Zheng, Y., He, K., and Zhang, Q.: Trends in China's anthropogenic emissions since 2010 as the consequence of clean air actions, Atmos. Chem. Phys., 18, 14 095–14 111, https://doi.org/10.5194/acp-18-14095-2018, 2018.